

THE EFFECTS OF PRECYCLING ON THE  
STRENGTH OF FERROCEMENT

Earle Stanley Babcock

DODLEY KNOX LIBRARY  
NAVAL POSTGRADUATE SCHOOL

# NAVAL POSTGRADUATE SCHOOL

## Monterey, California



# THESIS

THE EFFECTS OF PRECYCLING ON THE  
STRENGTH OF FERROCEMENT

by

Earle Stanley Babcock

June 1975

Thesis Advisor:

E. A. McKinnon

Approved for public release; distribution unlimited.

T167961



Unclassified

SECURITY CLASSIFICATION OF THIS PAGE (When Data Entered)

REPORT DOCUMENTATION PAGE		READ INSTRUCTIONS BEFORE COMPLETING FORM
1. REPORT NUMBER	2. GOVT ACCESSION NO.	3. RECIPIENT'S CATALOG NUMBER
4. TITLE (and Subtitle)  The Effects of Precycling on the Strength of Ferrocement		5. TYPE OF REPORT & PERIOD COVERED Master's Thesis; June 1975
		6. PERFORMING ORG. REPORT NUMBER
7. AUTHOR(s)  Earle Stanley Babcock		8. CONTRACT OR GRANT NUMBER(s)
9. PERFORMING ORGANIZATION NAME AND ADDRESS  Naval Postgraduate School Monterey, California 93940		10. PROGRAM ELEMENT, PROJECT, TASK AREA & WORK UNIT NUMBERS
11. CONTROLLING OFFICE NAME AND ADDRESS  Naval Postgraduate School Monterey, California 93940		12. REPORT DATE June 1975
		13. NUMBER OF PAGES
14. MONITORING AGENCY NAME & ADDRESS (if different from Controlling Office)  Naval Postgraduate School Monterey, California 93940		15. SECURITY CLASS. (of this report)  Unclassified
		15a. DECLASSIFICATION/DOWNGRADING SCHEDULE
16. DISTRIBUTION STATEMENT (of this Report)  Approved for public release; distribution unlimited		
17. DISTRIBUTION STATEMENT (of the abstract entered in Block 20, if different from Report)		
18. SUPPLEMENTARY NOTES		
19. KEY WORDS (Continue on reverse side if necessary and identify by block number)  Fatigue  Ferrocement  Precycling		
20. ABSTRACT (Continue on reverse side if necessary and identify by block number)  Ferrocement is a composite material made up of cement mortar reinforced with a mesh of steel wire. Its non-homogeneity results in material characteristics which are peculiarly its own. In this study, the ferrocement specimens tested varied in the type of wire reinforcement used, as well as in the water content of the mortar. Stress versus cycles to failure curves were developed, and comparisons were made between the		





curves of different types of specimens. Bending and tensile strength tests were conducted after cyclic loading in order to gain insights on the effects of precycling. Finally, some comparisons were made which related the data from this thesis to that of several preceding studies.





The Effects of Precycling on the  
Strength of Ferrocement

by

Earle Stanley Babcock  
Ensign, United States Navy  
B.S.M.E., United States Naval Academy, 1974

Submitted in partial fulfillment of the  
requirements for the degree of

MASTER OF SCIENCE IN MECHANICAL ENGINEERING

from the

NAVAL POSTGRADUATE SCHOOL

June 1975



## ABSTRACT

Ferrocement is a composite material made up of cement mortar reinforced with a mesh of steel wire. Its non-homogeneity results in material characteristics which are peculiarly its own. In this study, the ferrocement specimens tested varied in the type of wire reinforcement used, as well as in the water content of the mortar. Stress versus cycles to failure curves were developed, and comparisons were made between the curves of different types of specimens. Bending and tensile strength tests were conducted after cyclic loading in order to gain insights on the effects of precycling. Finally, some comparisons were made which related the data from this thesis to that of several preceding studies.



## TABLE OF CONTENTS

I.	INTRODUCTION-----	12
II.	BACKGROUND-----	13
III.	FABRICATION OF FERROCEMENT TESTING SPECIMENS-----	15
	A. GENERAL-----	15
	B. WIRE MESH REINFORCEMENT-----	15
	C. FABRICATION FORMS-----	16
	D. MORTAR-----	17
	E. CURING-----	17
	F. CUTTING PROCEDURE-----	18
	G. SPECIMEN IDENTIFICATION FORMAT-----	18
IV.	FATIGUE TESTS-----	19
	A. GENERAL-----	19
	B. APPARATUS-----	19
	C. SPECIMENS TESTED-----	20
	D. RESULTS AND DATA ANALYSIS-----	21
	E. CONCLUSIONS-----	22
V.	CYCLIC DEPENDENCY OF FLEXURAL STRENGTH-----	24
	A. GENERAL-----	24
	B. APPARATUS-----	24
	C. SPECIMENS TESTED-----	25
	D. RESULTS AND DATA ANALYSIS-----	25
	E. CONCLUSIONS-----	27
VI.	CYCLIC DEPENDENCY OF TENSILE STRENGTH-----	28
	A. GENERAL-----	28



B.	APPARATUS-----	28
C.	SPECIMENS TESTED-----	29
D.	RESULTS AND DATA ANALYSIS-----	29
E.	CONCLUSIONS-----	30
VII.	DATA TRENDS-----	32
A.	GENERAL-----	32
B.	CORRELATION OF S-N CURVES-----	32
C.	COMPARISON OF STRENGTH DATA-----	33
D.	CONCLUSIONS-----	34
VIII.	CONCLUSIONS AND RECOMMENDATIONS-----	35
A.	CONCLUSIONS-----	35
B.	RECOMMENDATIONS-----	36
	APPENDIX A: SPECIMEN IDENTIFICATION SYSTEMS-----	38
	APPENDIX B: CALCULATIONS-----	41
	APPENDIX C: TABLES-----	47
	APPENDIX D: FIGURES-----	52
	LIST OF REFERENCES-----	88
	INITIAL DISTRIBUTION LIST-----	90





## LIST OF TABLES

I.	Proportions for 0.45 Water/Cement Mortar for One Ferrocement Panel-----	47
II.	Results of Slump Tests and Compression Tests-----	47
III.	Results of Sieve Analysis-----	48
IV.	Bending Data-----	49
V.	Tensile Testing Data-----	50
VI.	Slopes of S-N Curves-----	51
VII.	Comparison of Strength Data-----	51



## LIST OF FIGURES

1.	Fabrication Frame with Wire Mesh-----	52
2.	Compression Cylinder with Capping Form-----	52
3.	Compression Cylinder after Testing-----	53
4.	Saw for Cutting Panels-----	53
5.	Fatigue Testing Jig-----	54
6.	Typical Fatigue Failure-----	54
7.	S-N Plot for Panel V-U45A-----	55
8.	S-N Plot for Panel V-U45B-----	56
9.	S-N Plot for Panel IV-G45A-----	57
10.	S-N Plot for Panel V-G45A-----	58
11.	S-N Plot for Panel III-G45C-----	59
12.	S-N Plot for Panel II-U40A-----	60
13.	S-N Plot for Panel II-G35A-----	61
14.	S-N Plot for Series 1PSU-----	62
15.	S-N Plot for Series 4ESU-----	63
16.	S-N Plot for Series 1PSG-----	64
17.	S-N Plot for Series 4ESG-----	65
18.	S-N Plot for Panel QUL7S3-----	66
19.	S-N Plot for Panel QUT7S2-----	67
20.	S-N Plot for Panel QUB7S1-----	68
21.	S-N Plot Comparing Results of Panels IV-G45A, V-G45A, and III-G45C-----	69
22.	S-N Plot Comparing Results of Panels V-U45A, V-U45B, and II-U40A-----	70
23.	S-N Plot Comparing Results of Panels IV-G45A, V-G45A, and II-G35A-----	71



24.	Monotonic Bending Apparatus-----	72
25.	Typical Monotonic Bending Failure-----	72
26.	Stress-Deflection Curves for Specimens V-U45B-10 and V-U45B-11 (No Precycling)-----	73
27.	Stress-Deflection Curves for Specimens V-U45B-8, V-U45B-9, and V-U45B-12 (33% Precycling)-----	74
28.	Stress-Deflection Curves for Specimens V-U45B-6 and V-U45B-7 (66% Precycling)-----	75
29.	Stress-Deflection Curves for Specimens V-G45A-8 and V-G45A-9 (No Precycling)-----	76
30.	Stress-Deflection Curves for Specimens V-G45A-6 and V-G45A-7 (33% Precycling)-----	77
31.	Stress-Deflection Curves for Specimens V-G45A-4 and V-G45A-5 (66% Precycling)-----	78
32.	Yield Strength and Ultimate Strength vs. Percentage of Precycling for Panel V-U45B-----	79
33.	Yield Strength and Ultimate Strength vs. Percentage of Precycling for Panel V-G45A-----	80
34.	Tinius-Olsen Testing Machine with Tensile Specimen in Place-----	81
35.	Tensile Specimen Showing Epoxy/Paper Coating and Tensile Failure Crack-----	81
36.	Unusual 3-Plane Tensile Failure-----	82
37.	Tensile Strength vs. Percentage of Precycling for Panel V-U45A-----	83
38.	Tensile Strength vs. Percentage of Precycling for Panel IV-G45A-----	84
39.	S-N Plot Comparing Results of All Panels with Ungalvanized Wire Reinforcement-----	85
40.	S-N Plot Comparing Results of Panels V-U45A, V-U45B, II-U40A, IPSU, and 4ESU-----	86
41.	S-N Plot Comparing Results for All Panels with Galvanized Wire Reinforcement-----	87





## LIST OF SYMBOLS AND ABBREVIATIONS

### Symbols

S	Stress
$S_y$	Monotonic Bending Yield Strength
$S_u$	Monotonic Bending Ultimate Strength
$S_{tu}$	Ultimate Tensile Strength
N	Number of Cycles to Fatigue Failure

### Abbreviations

psi	Pounds-Force per Square Inch
in	Inch
lbf	Pounds-Force
cm	Centimeter



## ACKNOWLEDGEMENT

The research supporting this thesis was undertaken in the various laboratories of the Department of Mechanical Engineering at the Naval Postgraduate School, Monterey, California. The help and advice of Mechanical Engineering Department professors and technicians contributed to successful completion of this study.

Acknowledgement is due to the following:

Dr. Kenneth Saczalski and the Office of Naval Research, for supporting this study;

Lt. David Sargent, who kindled my interest in ferrocement, and who helped me get started;

Ms. Anna May Schow, for the time and labor she put into the typing of this report.

Dr. Edwin A. McKinnon, who served as advisor for this thesis, is deserving of a special word of gratitude. His creativity, thoughtfulness, and encouragement, as well as his generosity with his time, were of inestimable value.

This thesis is dedicated to my wife, Karen, who remained steadfast and patient throughout its preparation.



## I. INTRODUCTION

Ferrocement is fabricated by impregnating layers of wire mesh with a cement mortar. The potential shapes and uses of ferrocement structures are limited only by the imagination of the designer. It is inexpensive when compared to such other structural materials as wood and steel.

Why, then, are there so few applications of this material in existence? One reason is the dearth of strength and fatigue data. To complicate the problem, existing ferrocement data generally exhibits extreme scatter from which it is difficult to draw specific conclusions.

The basic purpose of this study was to contribute as much as possible to the meager supply of ferrocement data. A number of fatigue tests were run which resulted in the formation of plots of stress versus cycles-to-failure. In addition, the effect of precycling ferrocement to predetermined percentages of fatigue life before flexural and tensile testing was investigated. The fatigue and strength data obtained for this study were compared to that of other studies in order to determine whether any general trends or similarities existed.



## II. BACKGROUND

Although extensive use of ferrocement is a fairly recent occurrence, the material has been in existence since 1848, when a Frenchman named Jean Louis Lambot[1]<sup>1</sup> created the first ferrocement boat hull. Recent interest in ferrocement has developed because of the material's suitability for construction of various types of small boat hulls. The use of ferrocement in hull construction was pioneered in England, Canada, and New Zealand [2, 3, 4, 5]. These initial maritime applications met with success. In addition, ferrocement's durability and low cost have made it increasingly attractive as a structural material. Haynes [6] and Simpson [7] discuss some of its current applications.

Ferrocement's increasing attractiveness created a need for reliable design data for this material. Existing reinforced concrete data is not generally applicable to ferrocement, which is a unique composite material; its characteristics are superior to those of the wire mesh or the mortar alone. The difference between reinforced concrete and ferrocement, as defined by Bezukladov [8], is based on the ratio of surface area of the reinforcement to the volume of the composite. Bezukladov [8] classified a material whose value of this ratio was  $2 \text{ cm}^{-1}$  or greater as ferrocement (the value of this ratio for the ferrocement used in this study was approximately  $10 \text{ cm}^{-1}$ ).

---

<sup>1</sup>Numbers in parentheses identify references; see pages 88-89.





Because reinforced concrete data is not applicable to ferrocement, extensive testing has resulted. Most of the systematic testing which has been done has been limited to monotonic testing methods [2, 3, 4, 5]. The variety of fabrication techniques, mortar ingredients, and curing methods makes standardization of ferrocement extremely difficult. Simpson [7] details many of the methods and materials currently in use.

Efforts have nonetheless been made to standardize fabrication and testing procedures, details of which are provided in references [2, 3, 4, 5]. Simpson [7] undertook the first detailed fatigue testing analysis of ferrocement. His findings were enhanced by those of Sargent [9], who used the same fabrication and testing procedures.



### III. FABRICATION OF FERROCEMENT TEST SPECIMENTS

#### A. GENERAL

The ferrocement specimens were made with the same facilities and procedures, in order to minimize data scatter. The approximate dimensions of each specimen were 18 inches long, 2-3/4 inches wide, and 1/2 inch thick. They were cut from panels which measured approximately 36 inches by 18 inches by 1/2 inch. The variations investigated were specimen age, type of wire mesh used, water content of the mortar, and type of cement used. All the specimens were steam cured.

#### B. WIRE MESH REINFORCEMENT

The wire mesh was cut from shipping rolls which were 50 feet long and 36 inches wide. The individual wires which composed the mesh each measured 0.040 inches in diameter. According to tests run by Simpson [7], each wire oriented perpendicular to the axis of the shipping roll had an ultimate strength of about 150,000 psi. Each wire parallel to the roll axis had an ultimate strength of approximately 114,000 psi. These wires were weaker because they were flash welded onto the longer wires, and became annealed at the points of attachment. The wire was cut into 18-inch by 36-inch sections, with the stronger wires 18 inches in length and the weaker wires 36 inches in length. In order to remove any oil, each layer of wire was soaked for a half hour in a heated solution of



2-1/2% by weight trisodium phosphate. Each layer was flattened with a sheet metal roller prior to mounting on the form.

### C. FABRICATION FORMS

The forms to which the layers of wire mesh were attached were made of 3/4-inch plywood cut into sections measuring approximately 20 inches by 40 inches. In order to prevent warping, each plywood section was attached to a rigid frame made of 2-inch by 4-inch fir. Once a plywood section was secured to its respective fir frame, a sheet of plastic was stretched over it and stapled into the frame. This was done in order to provide a smooth surface for the cement to dry on. It also acted as a vapor barrier between the mortar and the plywood.

The next step was the stapling of the wire mesh to the plywood. In each case, the first three layers were mounted with the 18-inch wires facing down, and the other four layers with the 18-inch wires facing up. This meant that the stronger wires were adjacent to both surfaces of each individual specimen. After each layer was secured, fine stainless steel wires were inserted through a series of small holes, which had been predrilled through the plywood. This served to hold the mesh tightly against the frame. After curing, these wires were cut to facilitate removal of the completed ferrocement panel. The final step of frame preparation was the nailing of wooden strips around the edges of the plywood panel. These strips were thick enough to keep the mortar from running off the frame. Figure 1 shows a typical frame prior to application of mortar.





#### D. MORTAR

Three different types of cement were used in the specimens considered in this study: Portland type II, Portland type V, and Kaiser CHEMCOMP. The other ingredients were washed and dried beach or quarry sand, pozzolan to replace the fine sand lost in the cleaning process, and water. Three ratios of water weight to cement weight were used in this study: 0.35, 0.40, and 0.45. In order to prevent gas production from electrolytic cell action, 300 parts per million of chromium trioxide was added, as recommended by Christensen and Williamson [10]. The mortar was mixed by hand in a wheelbarrow. The exact proportions of the ingredients are given in Table I, with the weights being accurate to the nearest 1/20th of a pound. Figures 2 and 3 show a typical compression cylinder before and after testing, respectively. Results of slump tests and compression tests, which were run according to ASTM standards [11], are given in Table II. Results of a sieve analysis run on a sample of the sand are shown in Table III. The mortar was troweled into the wire mesh, and a pencil vibrator used to insure adequate mortar penetration.

#### E. CURING

Steam curing was chosen for this study because it required about 26 hours of time, as compared to 28 days for water curing. Each panel was placed in a plastic, rectangular curing tent, which measured approximately 5 feet by 5 feet by 8 feet. During the first four hours, the temperature in the tent was



gradually brought up from ambient to 160<sup>0</sup> F. The temperature was maintained at 160<sup>0</sup> F for 18 hours, then gradually reduced to ambient over a four-hour period.

#### F. CUTTING PROCEDURE

The saw shown in Figure 4 was used to cut each ferrocement panel. The saw blade had a diamond impregnated tungsten carbide edge. All the cuts were made parallel to the 18-inch dimension of each panel. The number of specimens cut from each panel varied from 10 to 12.

#### G. SPECIMEN IDENTIFICATION FORMAT

Much of the data presented in this study was gathered by other authors who conducted previous research in ferrocement. Unfortunately, each author used a different identification system. The specimens used came from a total of 14 different panels. A complete explanation of the three systems used to identify these 14 panels is given in Appendix A.



#### IV. FATIGUE TESTS

##### A. GENERAL

One of the purposes of this study was to obtain as much fatigue data as possible, and compare it with data collected by previous researchers. This chapter is an analysis of the fatigue data collected for this study. The comparison is made in a later chapter. The average number of points used to generate each of the flexural stress versus cycles to failure (S-N) curves was ten points, with the highest number of points being 29, and the lowest being five. A least-squares fit was used to produce each curve, and though the fatigue limit was not deduced, the slope of each S-N curve and the data scatter were noted.

##### B. APPARATUS

The fatigue testing was carried out on a Baldwin Locomotive Works, Sonntag Model SF-1U fatigue testing machine. The individual specimens were mounted on the jig shown in Figure 5. No preload was set on any of the specimens, and the cycling frequency for all tests was 30 hertz. The stress levels in the specimens tested varied from as low as 650 psi to as high as 2250 psi. The method for calculating applied load is demonstrated in Appendix B, part 1. The accuracy of the applied load was  $\pm 0.5$  pounds. The actual load on each specimen took the form of a sinusoidally varying moment distributed evenly throughout an 8-inch center section.



Failure criterion was defined to be a maximum deflection of 1/2 inch. Most specimens undergoing this amount of deflection exhibited deep cracks in the proximity of the specimen's center, so most failures were plainly obvious to the naked eye. Figure 6 shows a typical fatigue failure. Micro-switches were mounted on the machine in order to automatically shut it off when the maximum deflection was reached. A cycle counter recorded the number of completed cycles to the last thousand. After the first few specimens failed, the micro-switches were re-adjusted to shut the machine down as soon as the specimen being tested underwent a deflection of 6/10 inch. Each time this was done, the machine shut down before executing an additional 1000 cycles, which justified the use of a deflection of 1/2 inch as the failure criterion.

### C. SPECIMENS TESTED

A total of seven panels were used to provide fatigue testing specimens exclusively for this study. This included five specimens from panel V-U45A, five from panel V-U45B, seven from panel IV-G45A, and five from V-G45A. The remaining specimens from these panels were used for other types of tests. In addition, 10 specimens were used from panel III-G45C, 11 from panel II-U40A, and 12 from panel II-G35A. The data obtained from these specimens was supplemented with data obtained by two previous researchers at the Naval Postgraduate School. The data used from Simpson's [7] study was obtained from 29 specimens from series 1PSG, 22 from series 1PSU, 10 from series 4ESG, and 10 from series 4ESU. The data used from Sargent's







[9] study was obtained from six specimens from panel QUL7S3, six from panel QUB7S1, and six from panel QUT7S2.

#### D. RESULTS AND DATA ANALYSIS

As previously stated, most of the specimens cycled to failure had visibly cracked at the place of failure. To determine the failure stress as precisely as possible, the width and thickness of each specimen was remeasured at the place of failure. These measurements were accurate to within 0.01 inches. Knowing these measurements and the applied load, the failure stress, as well as its uncertainty, could be calculated by the methods shown in Appendix B, parts 1 and 7, respectively. Each data point was plotted on semi-logarithmic graph paper, and a digital computer program designed to obtain a first order least-squares curve fit for a given set of data was utilized to obtain the S-N curves shown in Figures 7-20. There is an S-N curve for each of panels V-U45A, V-U45B, IV-G45A, V-G45A, III-G45C, II-U40A, and II-G35A. (Also included are the S-N curves developed by Simpson [7] and Sargent [9], which will be discussed in a later chapter.) Because Simpson [7] found that ungalvanized reinforcement led to longer fatigue life than galvanized reinforcement, it was expected that the curves for panels V-U45A, V-U45B, and II-U40A would be generally higher than the curves for the galvanized wire reinforced panels, and this proved to be the case. The effect of specimen age, as determined by comparing curves IV-G45A and V-G45A with curve III-G45C (see Figure 21) seemed to be that the older ferrocement had roughly the same fatigue life as new



ferrocement at stress levels of about 1500 psi and above. However, at lower stress levels the fatigue life of the older specimens appeared to drop off sharply. The effect of lower water content is inconclusive. The fatigue life at a given stress level for curves V-U45A and V-U45B is approximately an order of magnitude greater than the fatigue life at the same stress level for 11-U40A (see Figure 22) which has a lower water content. It should be noted, however, that panel II-U40A was about 18 months older than V-U45A and V-U45B, and it also differed in type of cement used. Comparison of curve II-G35A with curves IV-G45A and V-G45A shows that the specimens with lower water content exhibited slightly greater fatigue life than the other two sets of specimens, as shown by Figure 23.

In most cases, the failure of these fatigue specimens was pronounced, that is, a visible crack appeared at the place of failure. The exceptions occurred at high stress levels with fatigue lives of less than 100,000 cycles. Some of the specimens from the panels made from the Kaiser cement (II-U40A and II-G35A) did not exhibit any cracking whatsoever at these stress levels, even though they were deflecting sufficiently to satisfy the failure criterion.

#### E. CONCLUSIONS

The S-N curves developed for this study were consistent with expectations as far as fatigue strength versus type of reinforcement is concerned. They substantiated Simpson's [7] finding that ungalvanized mesh provides better reinforcement



than galvanized mesh. Age seemed to effect the fatigue life of ferrocement by shortening it at lower stress levels. The effects of the difference in water content were inconclusive. Using Kaiser cement in the mortar instead of Portland type II, resulted in the virtual elimination of cracking due to fatigue failure at high stress levels. With the exception of panel II-U40A, the scatter in the data is relatively small, considering the non-homogeneity of the material.



## V. CYCLIC DEPENDENCY OF FLEXURAL STRENGTH

### A. GENERAL

The primary objective of the bending tests undertaken in this study was to determine the effects of precycling on the ultimate and yield strengths of ferrocement. The S-N curves developed in the fatigue tests were used to determine the stress at which the test specimens were to be precycled. Several specimens were cycled to 33% of the fatigue life at this stress, and several were cycled to 66% of the fatigue life. They were then tested on the bending apparatus, along with several specimens which were not precycled at all. Stress versus deflection curves were developed from these tests, thus facilitating determination of precycling effects.

### B. APPARATUS

The specimens were loaded in pure bending by a Baldwin Locomotive Works compressive loading machine. The test specimens were mounted in the configuration shown in Figure 24. The loading rate was approximately 300 pounds per minute. Loading was applied continuously until the ultimate strength was reached. Deflection was measured by a dial indicator, and the load was recorded at each 0.05 inch deflection interval. The width and thickness of each specimen was measured, and the flexural bending stress was calculated using simple beam theory as shown in Appendix B, part 2.





### C. SPECIMENS TESTED

A total of 13 specimens were tested. Of these, seven were reinforced with ungalvanized wire. Five of these seven specimens were precycled at 1850 psi. This stress level was chosen because the S-N curve for panel V-U45B indicated that the fatigue life at this stress level was approximately 300,000 cycles, which was a convenient number to divide by three in order to obtain approximations of 33% and 66% of the fatigue life. Therefore, specimens V-U45B-8, -9, and -12 were cycled 100,000 times at 1850 psi and specimens V-U45B-6 and -7 were cycled 200,000 times at 1850 psi. Specimens V-U45B-10 and -11 were not precycled. The remaining six test specimens were reinforced with galvanized wire. Four of these six were precycled at 1250 psi, which was the stress level at which the fatigue life, according to the S-N curve for panel V-G45A, was about 300,000 cycles. Specimens V-G45A-4 and -5 were cycled 200,000 times, V-G45A-6 and -7 were cycled 100,000 times, and V-G45-8 and -9 were not precycled.

### D. RESULTS AND DATA ANALYSIS

Figures 26 through 31 are graphs of flexural stress versus deflection for each specimen tested. The uppermost point of each curve represents the ultimate strength. In most cases, the ultimate strength was reached when the specimens reached a deflection of 0.7 inches. The starred (★) point on each curve represents the yield strength. The yield strength is the point at which the tangent modulus equals the secant modulus at ultimate strength. This definition was introduced



by Simpson [7], and was also used by Sargent [9]. Table IV is a list of the specimens subjected to bending, and it includes the percent precycling they experienced, their yield strengths, their ultimate strengths, and their ratios of yield strength to ultimate strength.

It was expected that those specimens from panel V-U45B would exhibit higher yield and ultimate strengths than those from panel V-G45A, because the results of the fatigue tests revealed that specimens with ungalvanized reinforcement had greater endurance. This expectation was borne out by experimental results. The yield and ultimate strengths of the specimens from panel V-U45B were, respectively, approximately 1500 psi and 2000 psi greater than the yield and ultimate strengths of the specimens from panel V-G45A. It was also expected that the ratio of yield strength to ultimate strength would be roughly 0.75, which is a figure that had been determined in previous studies [5, 9, 10]. The average value of this ratio for all the specimens tested for this study was 0.786, which is in satisfactory agreement with the results of the aforementioned studies [5, 9, 10].

It was further expected that those specimens which had been precycled would exhibit lower yield and ultimate strengths than those which had not been precycled. The data gathered in this study neither substantiates nor repudiates this expectation. Figures 32 and 33 are plots of yield strength and ultimate strength versus percentage of precycling. Figure 32, which is composed of data gathered from panel V-U45B, indicates



that precycling had virtually no effect on either yield strength or ultimate strength. There is a 3% reduction in ultimate strength per 33% precycling, and a 0% reduction in yield strength per 33% precycling. If it could be substantiated in another study, this result would be highly significant. If ferrocement would retain most of its yield strength throughout its life, designers could be confident in the endurance capabilities of their ferrocement structures. However, Figure 33, which shows data collected from specimens from panel V-G45A, exhibits a 10% reduction in ultimate strength per 33% precycling, and a 9% reduction in yield strength per 33% precycling. These contradictory data prevent satisfactory determination of the effects of precycling on the monotonic bending of ferrocement.

#### E. CONCLUSIONS

Bending data was consistent with that of previous studies in that those specimens with ungalvanized reinforcement possessed greater yield and ultimate strengths than those with galvanized reinforcement. In addition, the ratios of yield strength to ultimate strength exhibited by the specimens tested were in satisfactory agreement with ratios determined by previous studies. Effects of precycling on bending are inconclusive. More data is required before these effects can be satisfactorily determined.





## VI. CYCLIC DEPENDENCY OF TENSILE STRENGTH

### A. GENERAL

The primary objective of the tensile tests was similar to that of the bending tests; that is, it was desired to determine the effects of precycling on the tensile strength of ferroce-ment. Here again, the S-N curves developed from the fatigue tests were used to determine the stress at which the test specimens were to be precycled. Some specimens were cycled to 66% of the fatigue life at this predetermined stress, some to 33% of the fatigue life, and the remainder were not pre-cycled. They were then tested in the tensile apparatus. Failure stress versus percentage of precycling curves were developed in order to graphically portray the precycling effects.

### B. APPARATUS

A Tinius-Olsen 200,000 pound testing machine was used to apply the tensile loads. Both ends of each specimen were firmly gripped in serrated jaws, as shown on Figure 34. The tensile load was then applied at a rate of approximately 1000 pounds per minute. Application of the load ceased when each specimen yielded, and the maximum load applied was recorded. The specimen was removed, and the width and thickness at the area of failure were measured. The ultimate tensile strength was then calculated using the procedure demonstrated in Appendix B, part 3.





### C. SPECIMENS TESTED

A total of 12 specimens underwent tensile testing, including seven with ungalvanized reinforcement and five with galvanized reinforcement. A stress level of 1850 psi was chosen for precycling of the specimens from panel V-U45A, because at this stress level the S-N curve predicted a fatigue life of 300,000 cycles. Specimens V-U45A-6 and -9 were cycled 100,000 times at 1850 psi, and specimens V-U45A-7 and -8 were cycled 200,000 times at the same stress level. Specimens V-U45A-10, -11, and -12 were not precycled. For the specimens from panel IV-G45A, a stress level of 1400 psi was chosen because the fatigue life was estimated to be 300,000 cycles. Again, this estimate was based on the S-N curve previously developed. Specimens IV-G45A-6 and -7 were cycled 100,000 times at 1400 psi, and specimen IV-G45-10 was cycled 200,000 times at the same stress level. Specimens IV-G45-11 and -12 were not precycled.

Prior to insertion of the test specimens into the jaws of the tensile testing machine, epoxy adhesive material was applied to the ends of each specimen. A piece of paper was pressed onto the epoxy to smooth out the surface. This entire procedure was carried out in order to ensure sufficient purchase of the test specimen by the jaws of the testing machine. Figure 35 shows a specimen after tensile testing.

### D. RESULTS AND DATA ANALYSIS

Table V is a presentation of the tensile testing data. Included in this table are values of tensile strength for each specimen tested, as well as ratios of tensile to yield



strength and tensile to ultimate strength. Sargent [9] found that these ratios showed the same relative values among the different specimens he tested as those determined from fatigue testing and monotonic bending. There was no such correlation here. Comparison of these ratios among the various specimens yielded no discernible pattern.

Comparison of tensile strengths between panel V-U45A and IV-G45A revealed that for a given percentage of precycling, the tensile strength of the specimens from panel V-U45A was from 300 psi to 600 psi greater than the tensile strength of the specimens from panel IV-G45A. This was consistent with the results of the fatigue testing.

Figure 37 is a graph of tensile strength versus percentage precycling for panel V-U45A. It was expected that precycling would tend to reduce tensile strength, and this expectation is borne out by this graph. The graph reveals that for each 33% of precycling, there is approximately a 10% drop in tensile strength. However, Figure 38, which is a graph of tensile strength versus percentage precycling for panel IV-G45A, reveals a slight increase in strength after 33% precycling, and an approximate 10% reduction in tensile strength after the next 33% of precycling. Again, the effort to conclusively determine the effects of precycling on ferrocement were thwarted because of contradictory data.

## E. CONCLUSIONS

The tensile tests conducted showed that ferrocement with ungalvanized wire reinforcement has a higher tensile strength



than does galvanized wire reinforcement. Ratios of tensile strength to yield strength and tensile strength to ultimate strength revealed no significant pattern. The tests run to determine the effects of precycling on the tensile strength of ferrocement proved to be inconclusive because of inconsistent data.



## VII. DATA TRENDS

### A. GENERAL

This thesis was a continuation of the work of two previous researchers at the Naval Postgraduate School. It was therefore felt that a correlation of all the data gathered might possibly reveal deeper insights into the nature of ferrocement. The purpose of this chapter is to report on some of the similarities of these three studies.

### B. CORRELATION OF S-N CURVES

Figures 14 through 17 show the S-N curves developed by Simpson [7], and figures 18 through 20 show the curves developed by Sargent [9]. As discussed in a previous chapter, the curves were obtained by entering the data into a computer program which computed a first order, least squares data fit. The computed results showed that the slopes of many of the curves were approximately equal. Table VI is a listing of the slopes of each of the S-N curves. Note that those panels reinforced with ungalvanized wire possess S-N curves which have roughly the same slope. Figure 39 shows a plot of all of these curves. Figure 40 shows another plot of these curves, excluding those curves developed by Sargent [9], which inadvertently underwent a discontinuous curing process. In addition, the wire orientations of his samples varied. Note that the five remaining curves, though they vary in water content and type of cement used, are almost exactly parallel.





The value of the average slope of these curves is -420 psi per decade of cycles, with a standard deviation of only 28 psi per decade of cycles.

This similarity of slope is a significant trend. Knowing the approximate slope of a given S-N curve would enable the researcher to get a reasonable idea of the nature of the S-N curve for a specific sample of ungalvanized wire reinforced, steam cured ferrocement. All that would be needed would be two or three data points in order to roughly determine the intercept, which, when combined with the known slope of -420 psi per decade of cycles, would yield an approximation of the desired S-N curve.

Figure 41 is a graph of all of the S-N curves which represent galvanized wire reinforced ferrocement. The slopes of these curves show no similarity. The most probable reason for this is lack of quality control in the galvanizing process, which results in non-uniformity of mesh strength.

#### C. COMPARISON OF STRENGTH DATA

Generally, the strength data taken for this study did not compare well with similar data taken by previous researchers. Table VII shows the average values found by each researcher for the yield strength, ultimate strength, and tensile strength of ungalvanized wire reinforced, steam cured ferrocement. Note that the values of yield strength and ultimate strength developed during this study are roughly 40% - 45% greater than the values developed by Simpson [7] and Sargent [9]. On the other hand, the tensile strength value found by Sargent [9] is



within 8% of the value determined in this study. (Simpson [7] took no tensile strength data.) The tensile strength data compares favorably, but there is an inconsistency in the yield strength and ultimate strength data.

#### D. CONCLUSIONS

Comparison of the S-N curves for ungalvanized wire reinforced, steam cured ferrocement developed by researchers at the Naval Postgraduate School exhibit remarkably similar slopes, which could represent a significant trend. Knowing the slope of an S-N curve would result in a good approximation of the curve, because only a few data points would be needed as intercepts. The S-N curves for ferrocement with galvanized wire reinforcement show no similarity in slope, which may well be due to the galvanizing process.

Though the tensile strength values compared favorably, the yield strength and ultimate strength values did not. This indicates that much more data is needed to produce satisfactory values for these strengths.



## VIII. CONCLUSIONS AND RECOMMENDATIONS

### A. CONCLUSIONS

As stated in the introductory chapter, the primary objectives of this study were to add as much as possible to the existing body of ferrocement fatigue data, and to investigate the effects of precycling on the yield, ultimate, and tensile strengths of this material. In addition, an investigation was to be made in order to determine whether data gathered by previous researchers at the Naval Postgraduate School, along with the data gathered for this study, exhibited any significant trends.

Data gathered for this study substantiated Simpson's [7] finding that the fatigue life, yield strength, and ultimate strength of ferrocement reinforced with ungalvanized wire were, respectively, significantly greater than fatigue life, yield strength, and ultimate strength for ferrocement reinforced with galvanized wire. Older ferrocement specimens exhibited shorter fatigue life at relatively low stress than new ferrocement, although the fatigue lives of both old and new ferrocement at stress levels of 1500 psi and greater were roughly the same. Mortar fabricated with Kaiser CHEMCOMP exhibited no cracking for fatigue failure at high stress levels, though all other specimens at all other stress levels exhibited the type of cracking shown in Figure 6.



The effects of precycling on the strength of ferrocement were not conclusively determined. Some of the data gathered indicated that precycling effects were negligible, while other data revealed a drop of roughly 10% in yield strength and ultimate strength per decade of precycling.

Comparison of the S-N curves developed by previous researchers with those developed for this study revealed a significant similarity of slope among the curves for ungalvanized wire reinforced ferrocement. The slopes of the S-N curves for galvanized wire reinforced ferrocement exhibited a great degree of scatter, which is probably the result of poor quality control in the galvanizing process.

The values of yield strength and ultimate strength for various types of ferrocement differed significantly. The values of these strengths developed for this study were roughly 40% greater than the values found by Sargent [9] and Simpson [7], although the ratio of yield strength to ultimate strength for all the data gathered was roughly 0.75. The scatter in these strength values is probably the result of some variance in the fabrication process. Such variables as ambient temperature, wire mesh roll used, baking time of sand, mesh rolling and cleaning processes, humidity, etc., could have combined to greatly affect the various test results.

## B. RECOMMENDATIONS

Further investigation into the effects of precycling is needed in order to conclusively determine these effects. In addition, much more data is needed in order to arrive at







accurate figures for flexural and tensile strengths. A large scale project in which each step of the fabrication process is closely controlled could greatly enhance existing knowledge concerning the strength of ferrocement. The effects of age and water content of the mortar could be further investigated, as could the effects of steel rod reinforcement coupled with the mesh reinforcement. Fatigue testing of specimens of varying size and shape has yet to be carried out. A study of different types of coatings would be beneficial. A series of tests conducted in a marine environment would no doubt yield interesting results. In short, there are many areas open in which meaningful research could be conducted. Reference [12] gives many sources which can provide background information for further study.



## APPENDIX A: SPECIMEN IDENTIFICATION SYSTEMS

Each ferrocement specimen is labeled in one of the following three ways:

1.  $X_1-X_2X_3X_4-X_5$
2.  $Y_1Y_2Y_3Y_4-Y_5$
3.  $Z_1Z_2Z_3Z_4Z_5Z_6-Z_7$

Explanations of each of these respective identification systems follow.

1.  $X_1-X_2X_3X_4-X_5$

$X_1$ :	Date of Panel Fabrication	II = August 21, 1973
		III = July 24, 1974
		IV = December 18, 1974
		V = January 5, 1975
$X_2$ :	Wire Type	G = Galvanized
		U = Ungalvanized
$X_3$ :	Percentage of Weight of Water to Cement	
$X_4$ :	Successive Letter Corresponding to Number of Panels of this Type	
$X_5$ :	Specimen Number; Identifies specimen cut from Larger Panel	

(All panels identified in the above manner were steam cured.)

Example: V-U45B identifies the second panel made on January 5, 1975, with ungalvanized wire reinforcement and an



0.45 water weight to cement weight ratio. V-U45B-6  
is the sixth specimen cut from the preceding panel.

2.  $Y_1Y_2Y_3Y_4-Y_5$  (This was the identification system used  
by Simpson [7])

$Y_1$ : Numeral identifying chronological  
order of series

$Y_2$ : Type of Cement

P = Portland Type V

E = Kaiser CHEMCOMP

$Y_3$ : Type of Curing

S = Steam

$Y_4$ : Wire Type

U = Ungalvanized

G = Galvanized

$Y_5$ : Specimen Number

Example: 1PSU is the first series of Portland type V, ungalvanized wire reinforced, steam cured ferrocement.  
1PSU-2 identifies the second specimen of the preceding series.

3.  $Z_1Z_2Z_3Z_4Z_5Z_6-Z_7$  (This was the identification system  
used by Sargent [9])

$Z_1$ : Type of Cement

Q = Portland Type II

$Z_2$ : Wire Type

U = Ungalvanized

$Z_3$ : Wire Orientation

L = Longitudinal (Long  
wires on roll are  
parallel to long  
dimension of  
specimen.)

T = Transverse (Short  
wires on roll run  
parallel to long  
dimension of  
specimen.)



B = Alternating (Layers alternate between L and T; outer layers are T orientation for odd number of layers.)

Z<sub>4</sub>: Number of Layers of Wire Mesh

Z<sub>5</sub>: Method of Curing                      S = Steam

Z<sub>6</sub>: Successive Number of Panels of  
this Type

Z<sub>7</sub>: Specimen Number

Example: QUL7S1 identifies the first panel made from Portland type II cement with ungalvanized wire reinforcement. All the long roll wires are parallel to the long dimension of the specimen, and the panel has been steam cured. QUL7S1-4 identifies the fourth specimen cut from the preceding panel.





## APPENDIX B: CALCULATIONS

### 1. Maximum Fatigue Flexure Stress

From simple beam theory:

$$S_f = \frac{Mh}{2I} = \frac{M h}{2 \left( \frac{bh^3}{12} \right)} = \frac{6M}{bh^2}$$

But,  $M = \frac{RP}{2} = 3P$  for testing apparatus of this study.

$$\text{Therefore, } S_f = \frac{18P}{bh^2}$$

where

$S_f$  = maximum flexural stress (psi)

$M$  = applied bending moment (lbf-in)

$P$  = amplitude of cyclic force applied by  
testing machine (lbf)

$R$  = moment arm of fatigue fixture (6 in)

$h$  = specimen thickness (in)

$b$  = specimen width (in)

$I$  = specimen cross-section moment of  
inertia (in<sup>4</sup>)



## 2. Monotonic Bending Stress

From simple beam theory:

$$S_{mb} = \frac{Mh}{2I} = \frac{6M}{bh^2}$$

But,  $M = \frac{RP}{2} = \frac{3P}{2}$  for apparatus used in this study.

$$\text{Therefore, } S_{mb} = \frac{9P}{bh^2}$$

where

$S_{mb}$  = maximum monotonic bending stress (psi)

$M$  = applied bending moment (lbf-in)

$P$  = force applied by testing machine (lbf)

$R$  = moment arm of monotonic bending fixture (3 in)

$h$  = specimen thickness (in)

$b$  = specimen width (in)

$I$  = specimen cross-section moment of inertia (in<sup>4</sup>)

## 3. Tensile Stress

$$S_t = \frac{P}{bh}$$

where

$S_t$  = tensile stress (psi)

$h$  = specimen thickness (in)

$b$  = specimen width (in)

$P$  = force applied by testing machine



#### 4. First Order Least Squares Approximation

It is assumed that all ferrocement S-N curves can be approximated by a first order polynomial of the form

$$y = a_0 + a_1x$$

where

$y$  = fatigue flexure stress (psi)

$x$  = logarithm of  $N$ , which is the fatigue life  
corresponding to stress  $y$

$a_0$  = intercept corresponding to  $N = 1$  (psi)

$a_1$  = slope of S-N curve (psi per decade of cycles)

Utilizing the algorithm presented by Dorn and McCracken [13]:

$$a_0 = \frac{\sum y_i \sum x_i^2 - \sum x_i \sum x_i y_i}{m \sum x_i^2 - \left( \sum x_i \right)^2}$$
$$a_1 = \frac{m \sum x_i y_i - \sum x_i \sum y_i}{m \sum x_i^2 - \left( \sum x_i \right)^2}$$

where

$y_i$  = "i"th fatigue flexure stress point

$x_i$  = logarithm of value of  $N$  corresponding to  $y_i$

$m$  = total number of data points



## 5. Standard Deviation

Standard deviation is defined as:

$$S.D. = \sqrt{\frac{\sum (x - \bar{x})^2}{N}}$$

where

$x$  = value of data point

$\bar{x}$  = average of data point values

$N$  = number of data points

## 6. Uncertainty Analyses

Kline and McClintock [14] have deduced the following general error equation:

$$\text{error in } X = \left[ \sum_{i=1}^n \left( \frac{\partial S w_i}{\partial x_i} \right)^2 \right]^{\frac{1}{2}}$$

where

$$X = f(x_1, x_2, x_3 \dots x_n)$$

$w_i$  = uncertainty in measurement of parameter  $x_i$

## 7. Uncertainty in Fatigue Flexure Stress

Uncertainty in  $S_f$

$$= \left[ \left( \frac{18w_p}{bh^2} \right)^2 + \left( \frac{18Pw_b}{b^2h^2} \right)^2 + \left( \frac{36Pw_h}{bh^3} \right)^2 \right]^{\frac{1}{2}}$$

Estimates of parameter error:

$w_p = 0.5 \text{ lbf} = \text{uncertainty in load}$

$w_b = 0.01 \text{ in} = \text{uncertainty in specimen width}$

$w_h = 0.01 \text{ in} = \text{uncertainty in specimen thickness}$





Using these estimates, the uncertainty in  $S_f$  is:

$$= \left[ \left( \frac{9}{bh^2} \right)^2 + \left( \frac{.18P}{b^2h^2} \right)^2 + \left( \frac{.36P}{bh^3} \right)^2 \right]^{\frac{1}{2}}$$

## 8. Uncertainty in Monotonic Bending Stress

Uncertainty in  $S_{mb}$

$$= \left[ \left( \frac{9w_p}{bh^2} \right)^2 + \left( \frac{9Pw_b}{b^2h^2} \right)^2 + \left( \frac{18Pw_h}{bh^3} \right)^2 \right]^{\frac{1}{2}}$$

Estimates of parameter error:

$$w_p = 1.0 \text{ lbf}$$

$$w_b = 0.01 \text{ in}$$

$$w_h = 0.01 \text{ in}$$

Using these estimates, the error in  $S_{mb}$  is:

$$= \left[ \left( \frac{9}{bh^2} \right)^2 + \left( \frac{.09P}{b^2h^2} \right)^2 + \left( \frac{18P}{bh^3} \right)^2 \right]^{\frac{1}{2}}$$

## 9. Uncertainty in Tensile Stress

Uncertainty in  $S_t$

$$= \left[ \left( \frac{w_p}{bh} \right)^2 + \left( \frac{Pw_b}{b^2h} \right)^2 + \left( \frac{Pw_h}{bh^2} \right)^2 \right]^{\frac{1}{2}}$$

Estimates of parameter error:

$$w_p = 1.0 \text{ lbf}$$

$$w_b = 0.01 \text{ in}$$

$$w_h = 0.01 \text{ in}$$



Using these estimates, the uncertainty in  $S_t$

$$= \left[ \left( \frac{1}{bh} \right)^2 + \left( \frac{.01P}{b^2h} \right)^2 + \left( \frac{.01P}{bh^2} \right)^2 \right]^{\frac{1}{2}}$$



## APPENDIX C: TABLES

Table I. Proportions for 0.45 Water/Cement Mortar  
for One Ferrocement Panel

Ingredient	Amount
Sand	2.2 lbs.
Pozzolon	0.55 lbs.
Cement	11.27 lbs.
Water	5.3 lbs.
CrO <sub>3</sub> (Conc.)	300 ppm

Table II. Results of Slump Tests and Compression Tests

Batch	Slump (in)	Compression Limit (psi)
II	2.5	4270
III	3.5	2700
IV	2.12	5550
V	4.0	4700



Table III. Results of Sieve Analysis

Tyler Standard Sieve Size	Percent Passing
8	100
10	99
14	88
16	73
20	64
28	38
32	32
35	26
48	13
80	0.5
150	Trace
200	0





Table IV. Bending Data

Specimen	% Precycling	$S_y$ (psi)	$S_u$ (psi)	$S_y/S_u$
V-G45A-8	0	4300	5420	0.793
V-G45A-9	0	4060	4940	0.822
V-G45A-6	33	4140	5080	0.815
V-G45A-7	33	3600	4050	0.889
V-G45A-4	66	4080	5020	0.813
V-G45A-5	66	2780	3450	0.806
V-U45A-10	0	5720	7820	0.731
V-U45A-11	0	5560	7500	0.741
V-U45A-8	33	5280	7000	0.754
V-U45A-9	33	5560	7540	0.751
V-U45A-12	33	5600	7660	0.731
V-U45A-6	66	5700	7220	0.789
V-U45A-7	66	5700	7220	0.789



Table V. Tensile Testing Data

Specimen	% Precycling	$S_{tu}$	$S_{tu}/S_y$	$S_{tu}/S_u$
V-U45B-10	0	2900	0.514	0.378
V-U45B-11	0	3200	0.567	0.417
V-U45B-12	0	2780	0.493	0.363
V-U45B-6	33	2480	0.450	0.335
V-U45B-9	33	2860	0.519	0.387
V-U45B-7	66	2540	0.445	0.352
V-U45B-8	66	2200	0.386	0.305
IV-G45A-11	0	2300	0.551	0.445
IV-G45A-12	0	2340	0.560	0.452
IV-G45A-6	33	2430	0.627	0.531
IV-G45A-7	33	2260	0.584	0.495
IV-G45A-10	66	2070	0.608	0.493



Table VI: Slopes of S-N Curves

Panel	Slope (psi per decade of cycles)
V-U45A	-440
V-U45B	-420
IV-G45A	-250
V-G45A	-210
III-G45C	-660
II-U40A	-380
II-G35A	-370
1PSU	-450
4ESU	-410
1PSG	-450
4ESG	-420
QUL7S3	-610
QUT7S2	-480
QUB7S1	-516

Table VII. Comparison of Strength Data

	Simpson	Sargent	Babcock
$S_y$ (psi)	3950	4040	5640
$S_u$ (psi)	5100	5380	7660
$S_{tu}$ (psi)	-	2810	3050



APPENDIX D: FIGURES



FIGURE 1. FABRICATION FRAME WITH WIRE MESH

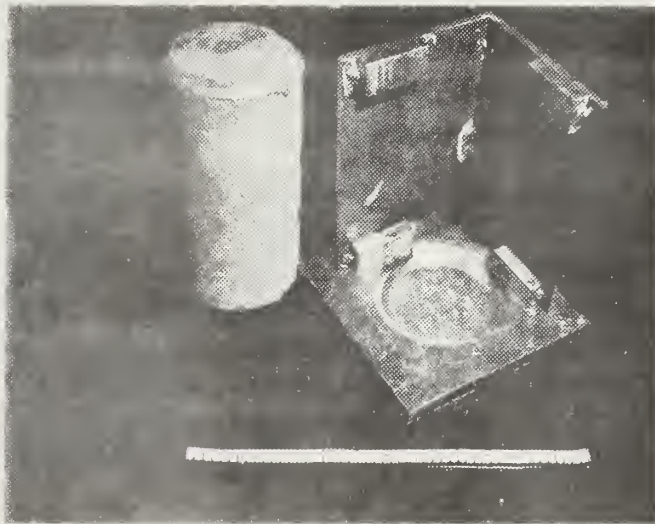


FIGURE 2. COMPRESSION CYLINDER WITH CAPPING FORM





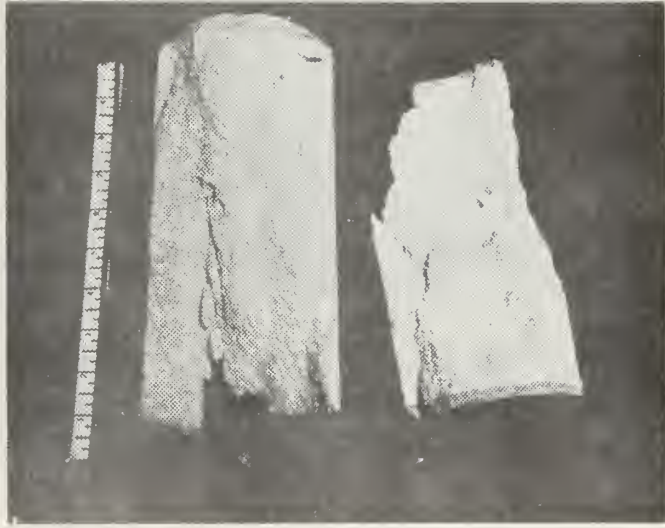


FIGURE 3. COMPRESSION CYLINDER AFTER TESTING

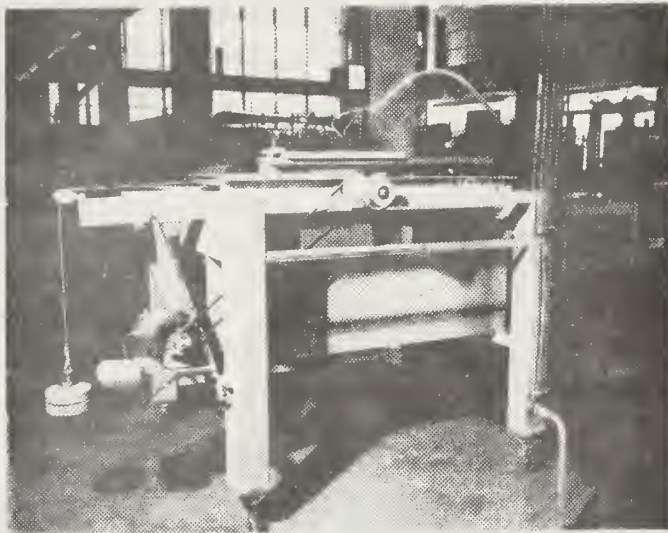


FIGURE 4. SAW FOR CUTTING PANELS



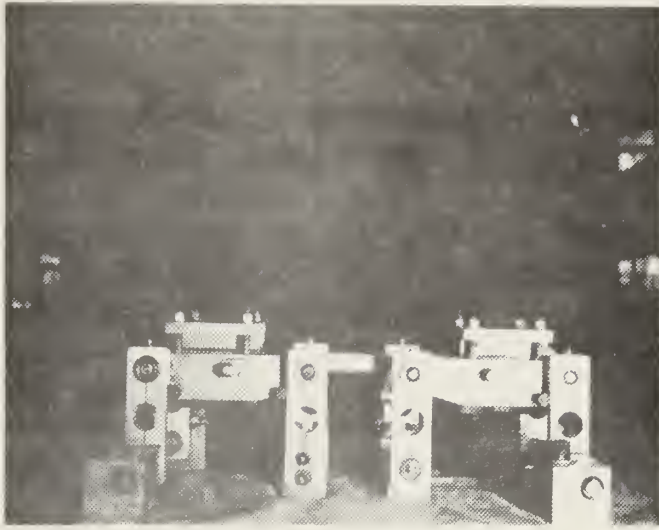


FIGURE 5. FATIGUE TESTING JIG

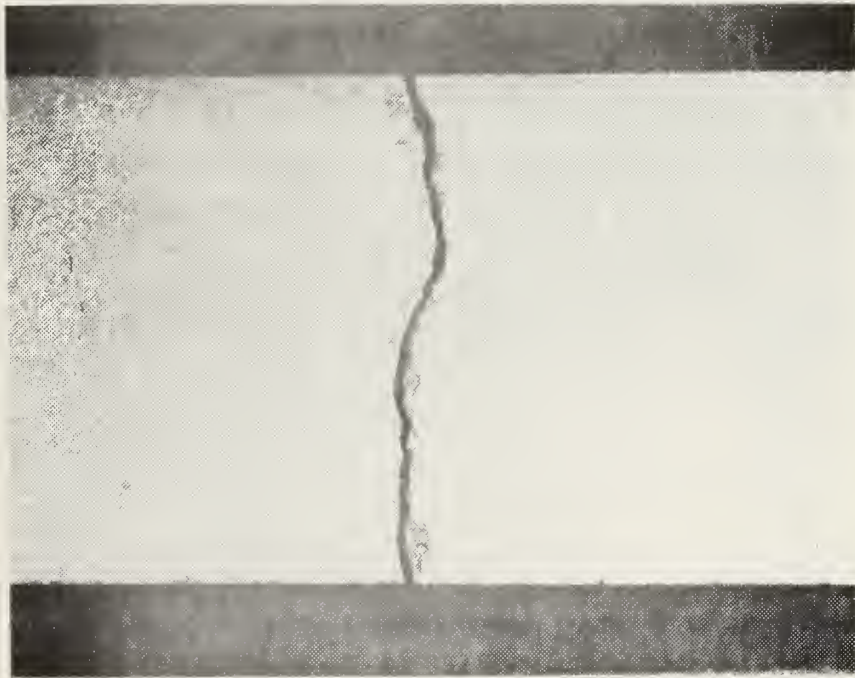


FIGURE 6. TYPICAL FATIGUE FAILURE



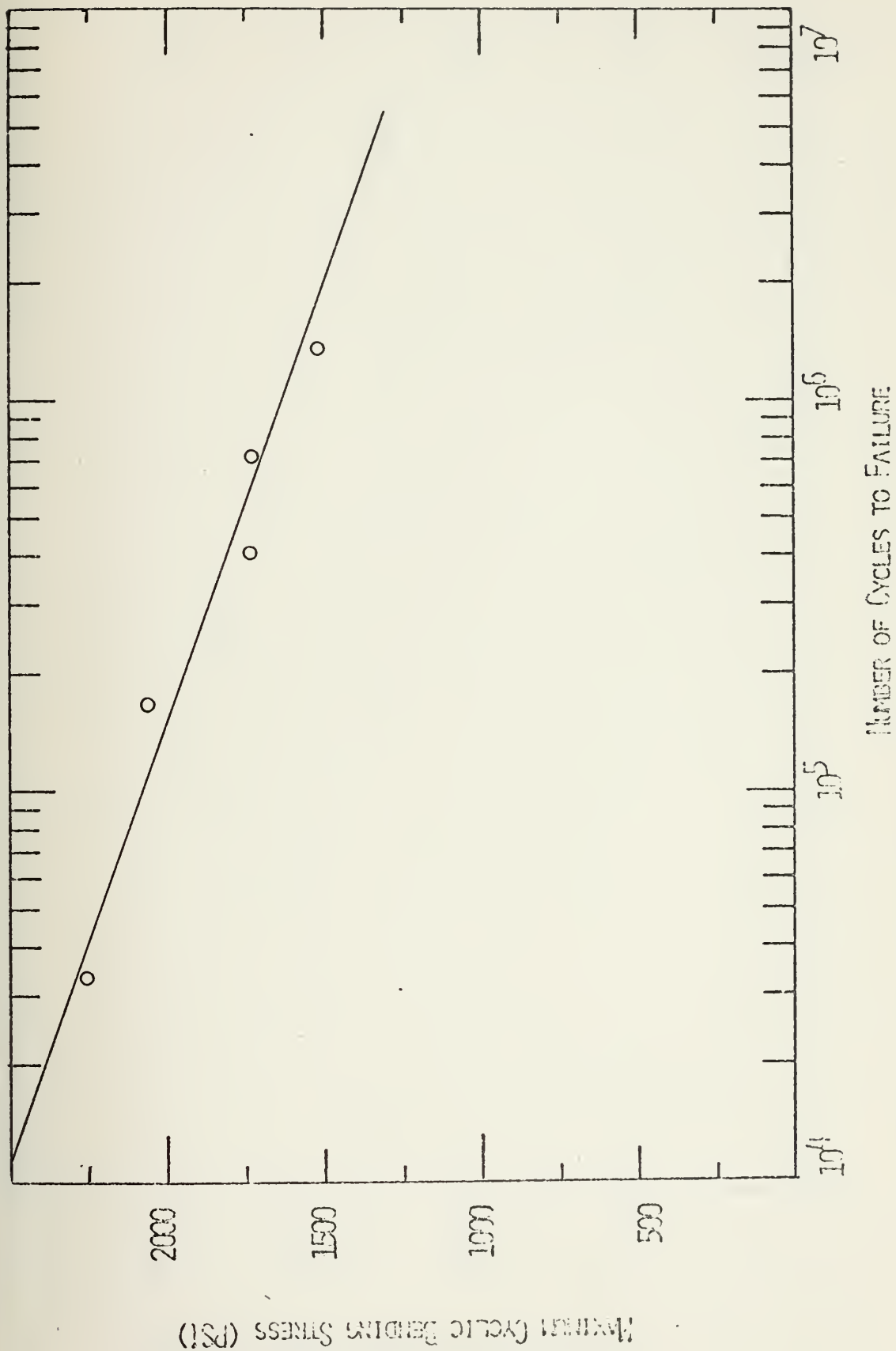


FIGURE 7. S-N PLOT FOR PANEL V-U45A



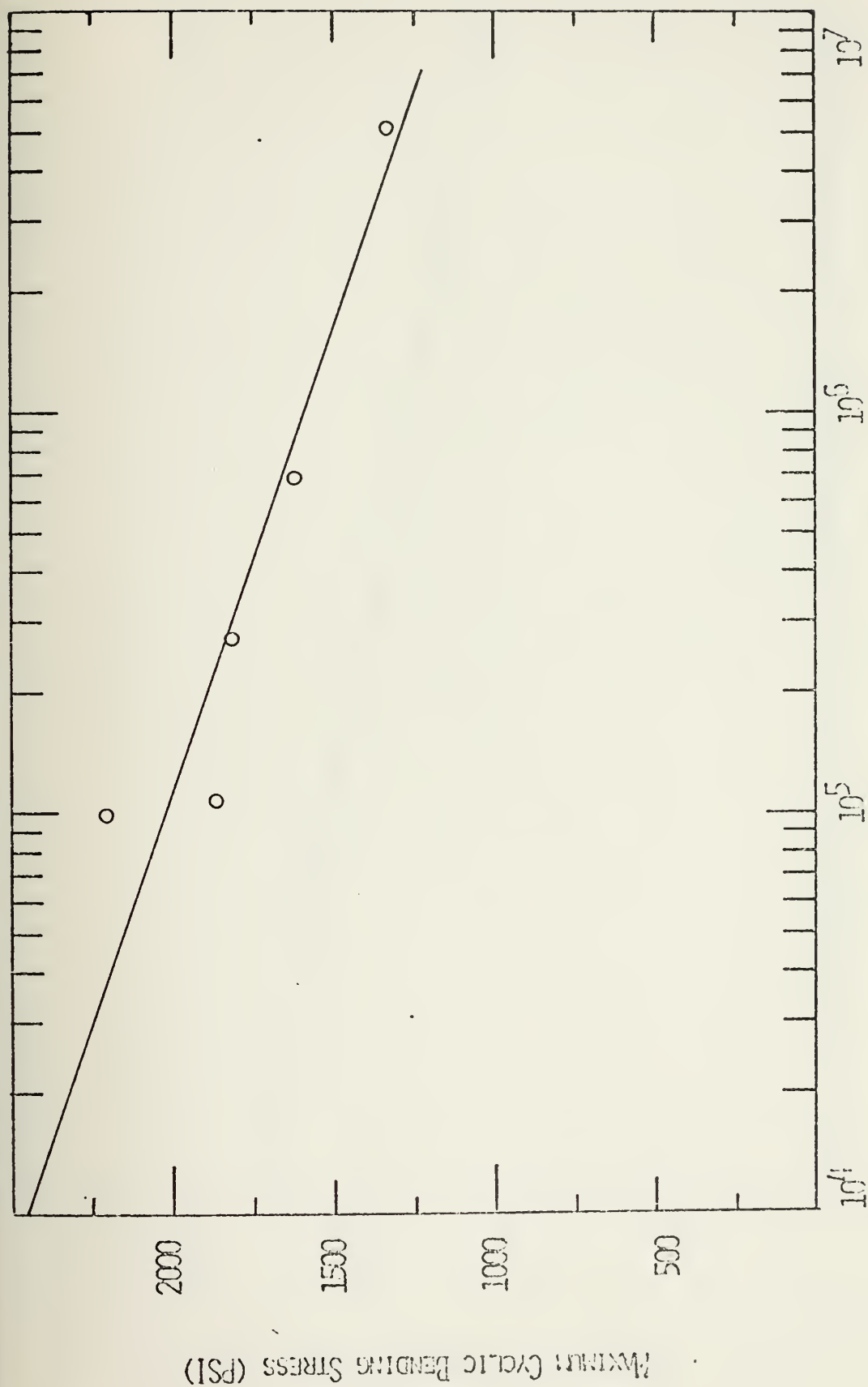


FIGURE 8. S-N PLOT FOR PANEL V-U45B





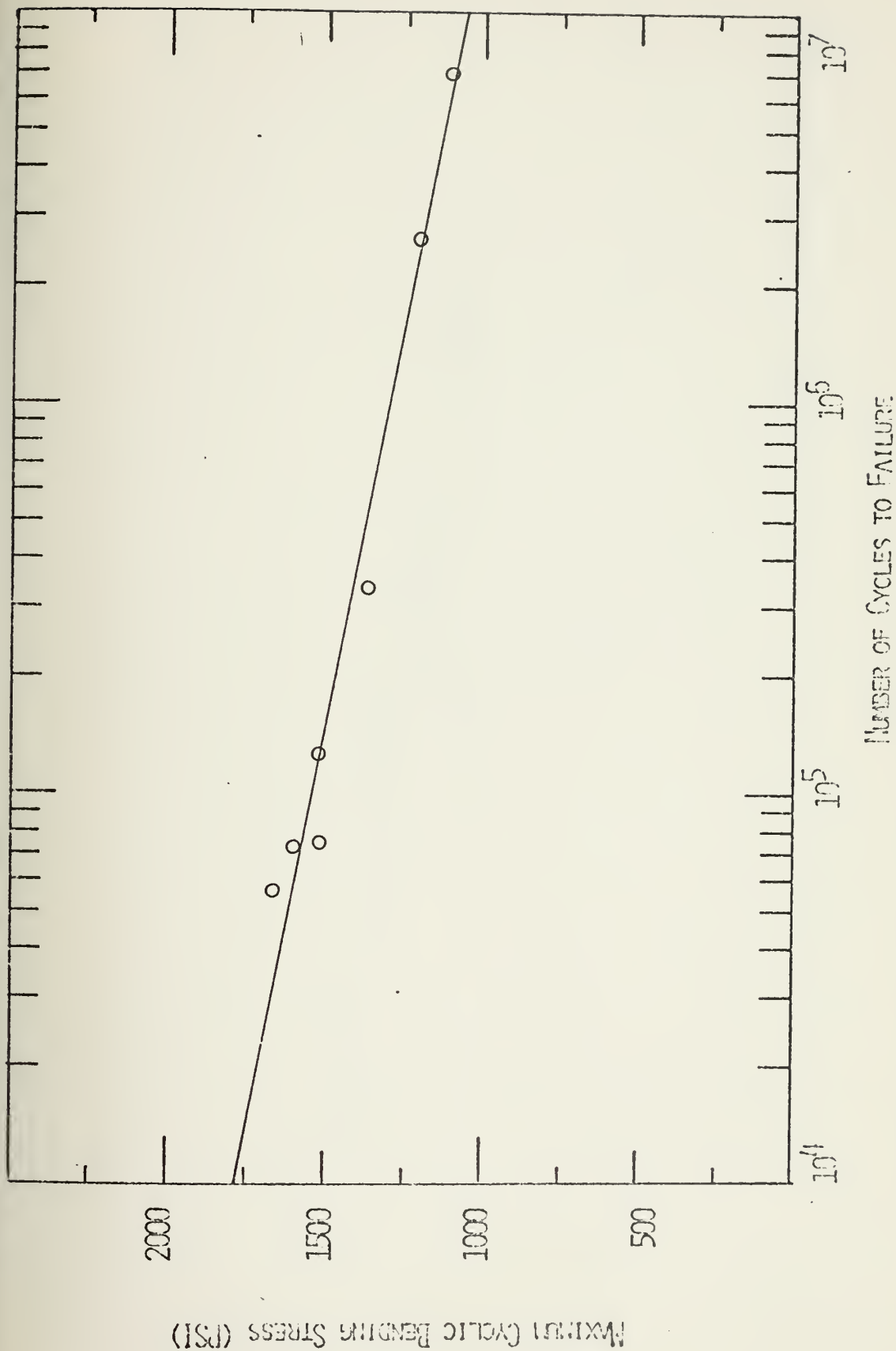


FIGURE 9. S-N PLOT FOR PANEL IV-G45A



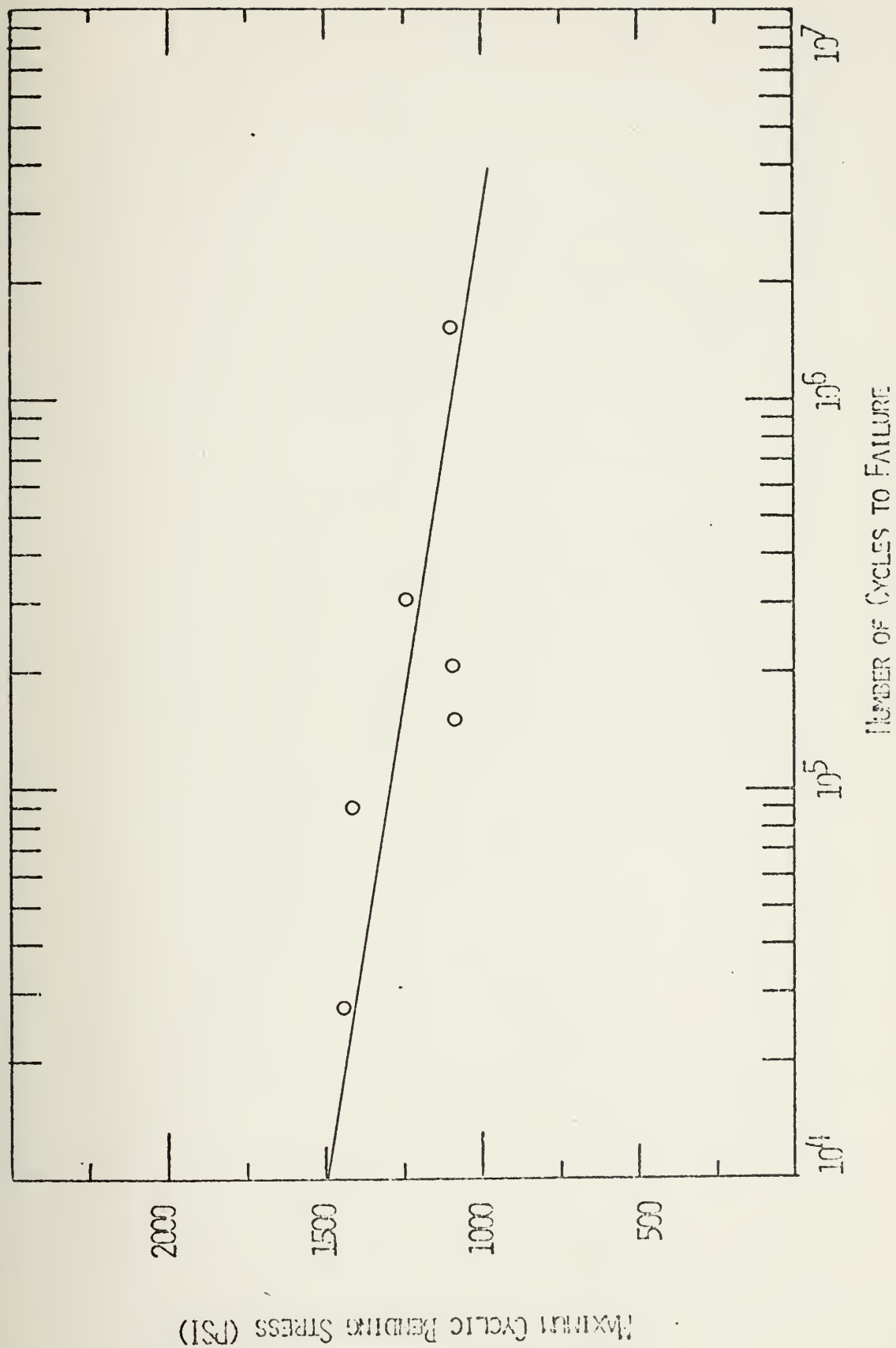


FIGURE 10. S-N PLOT FOR PANEL V-G45A



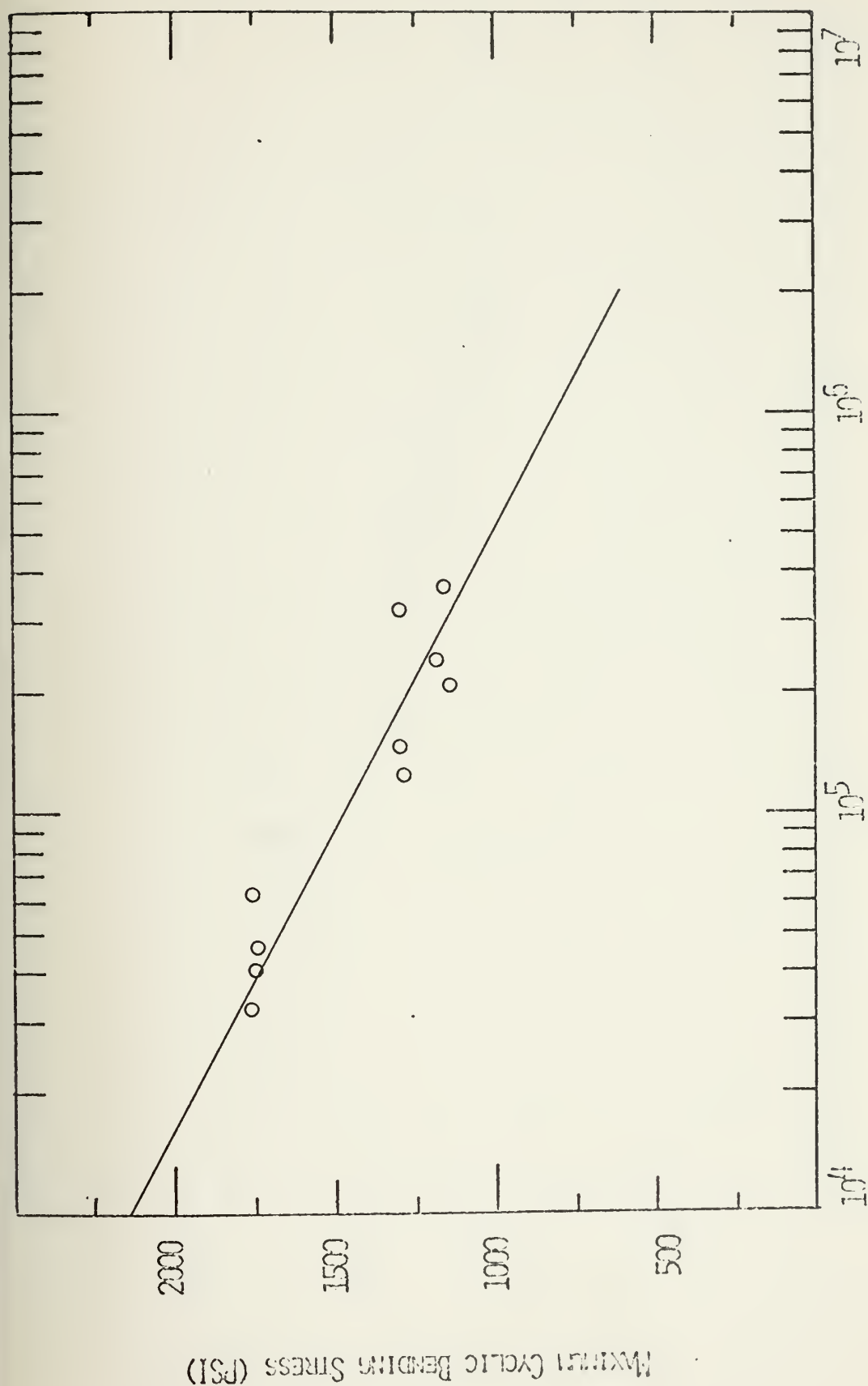


FIGURE 11. S-N PLOT FOR PANEL III-G45C



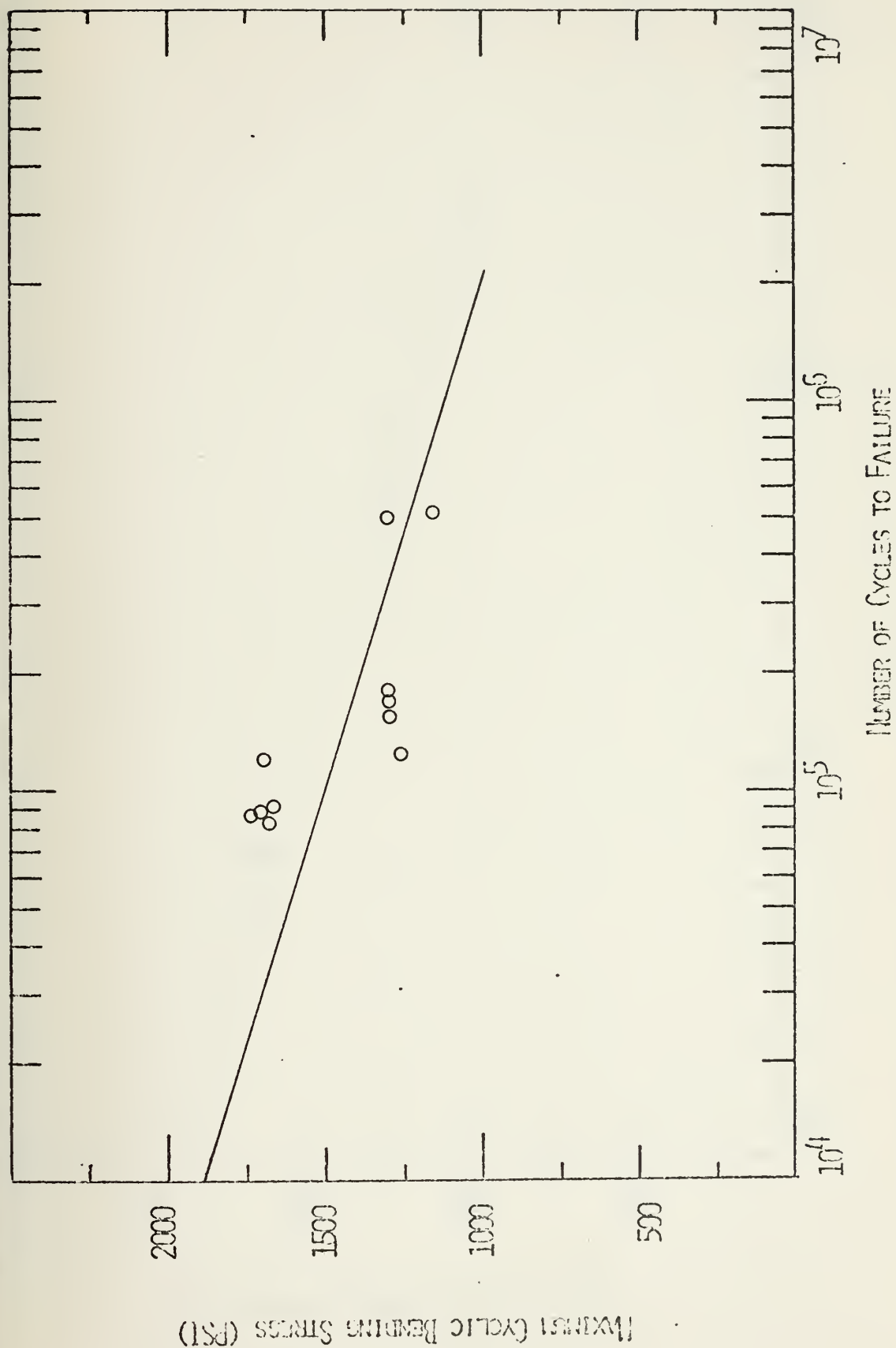


FIGURE 12. S-N PLOT FOR PANEL II-U40A





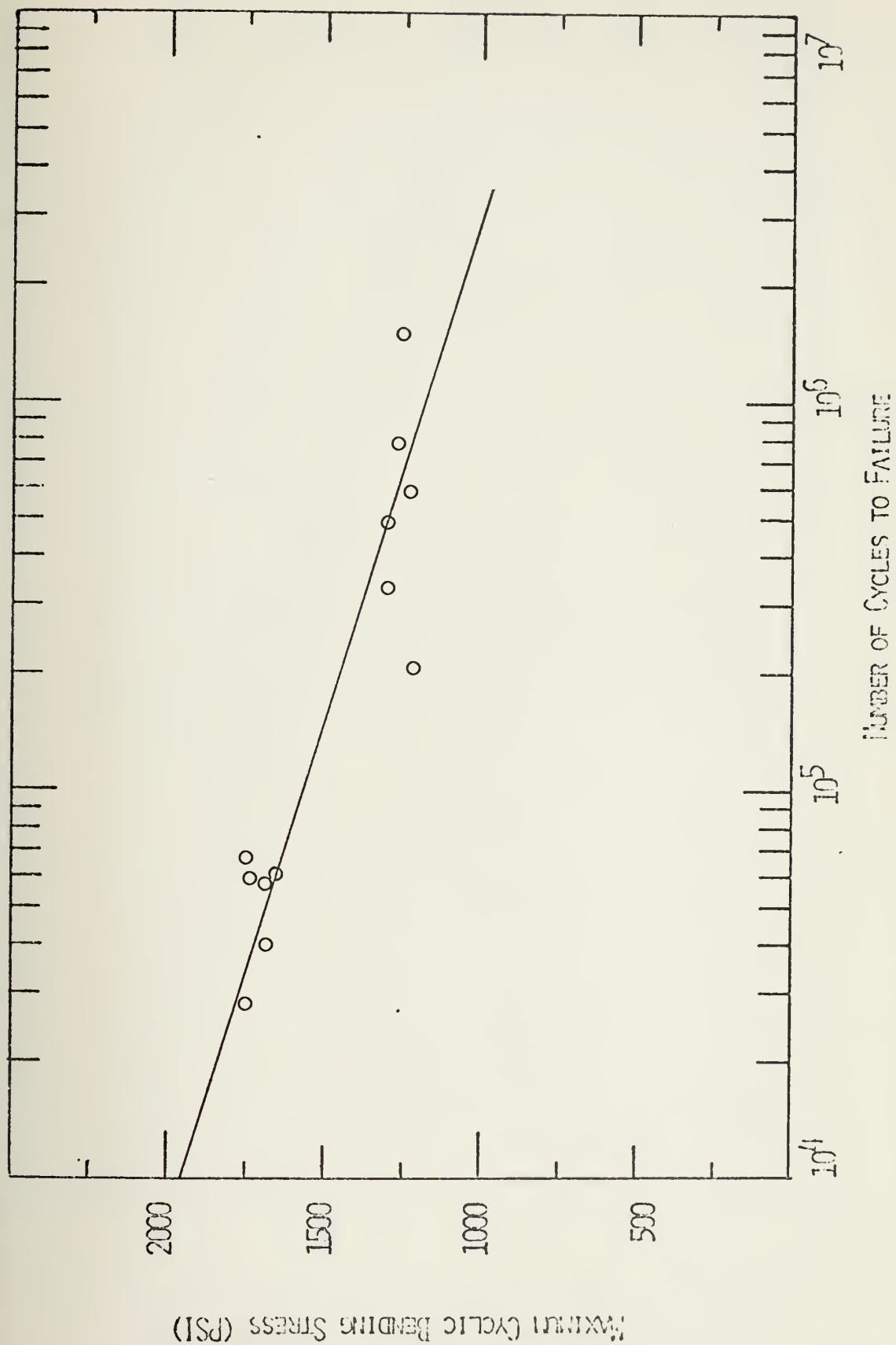
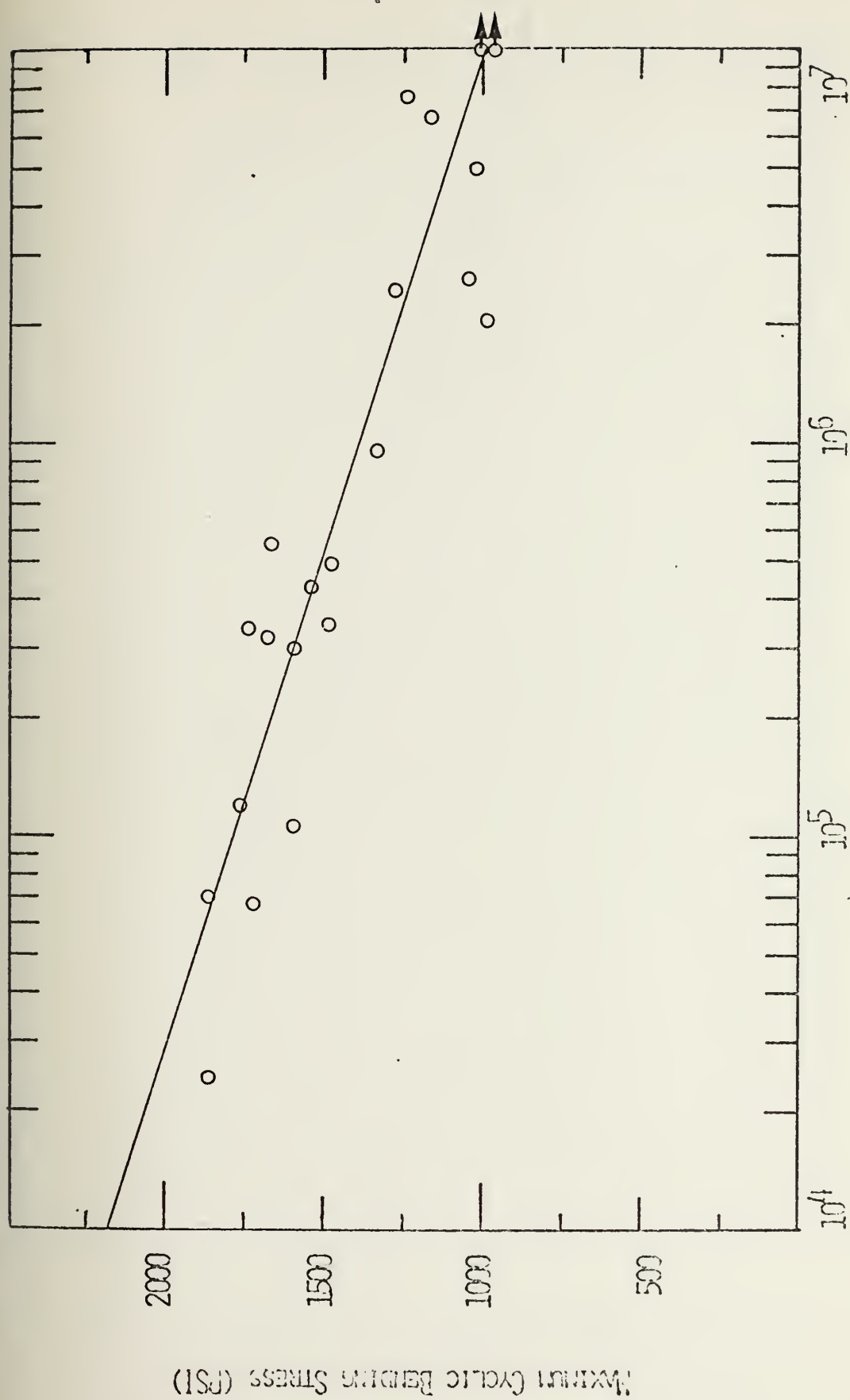


FIGURE 13. S-N PLOT FOR PANEL II-G35A





NUMBER OF CYCLES TO FAILURE

FIGURE 14. S-N PLOT FOR SERIES 1PSU



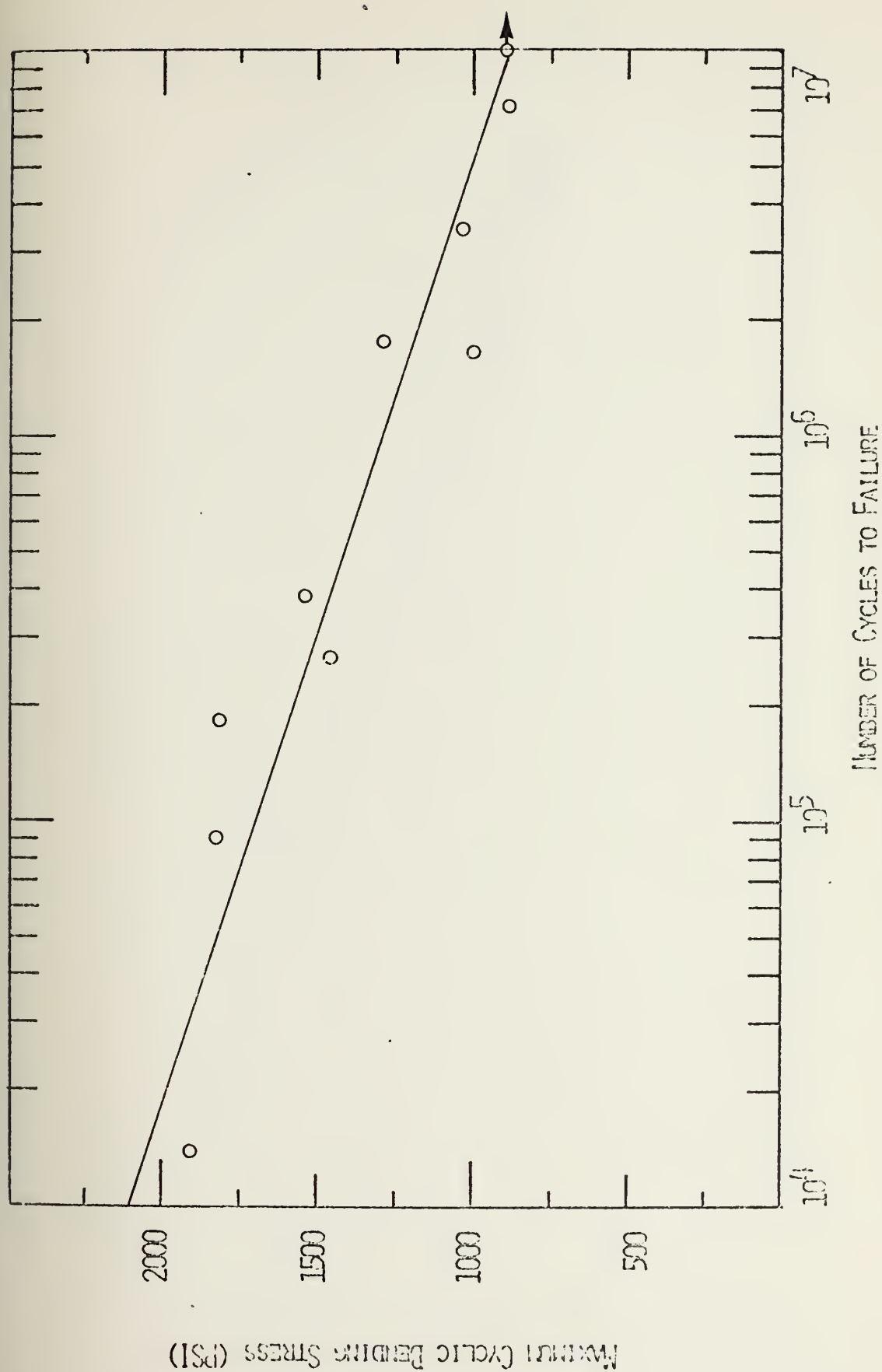


FIGURE 15. S-N PLOT FOR SERIES 4ESU



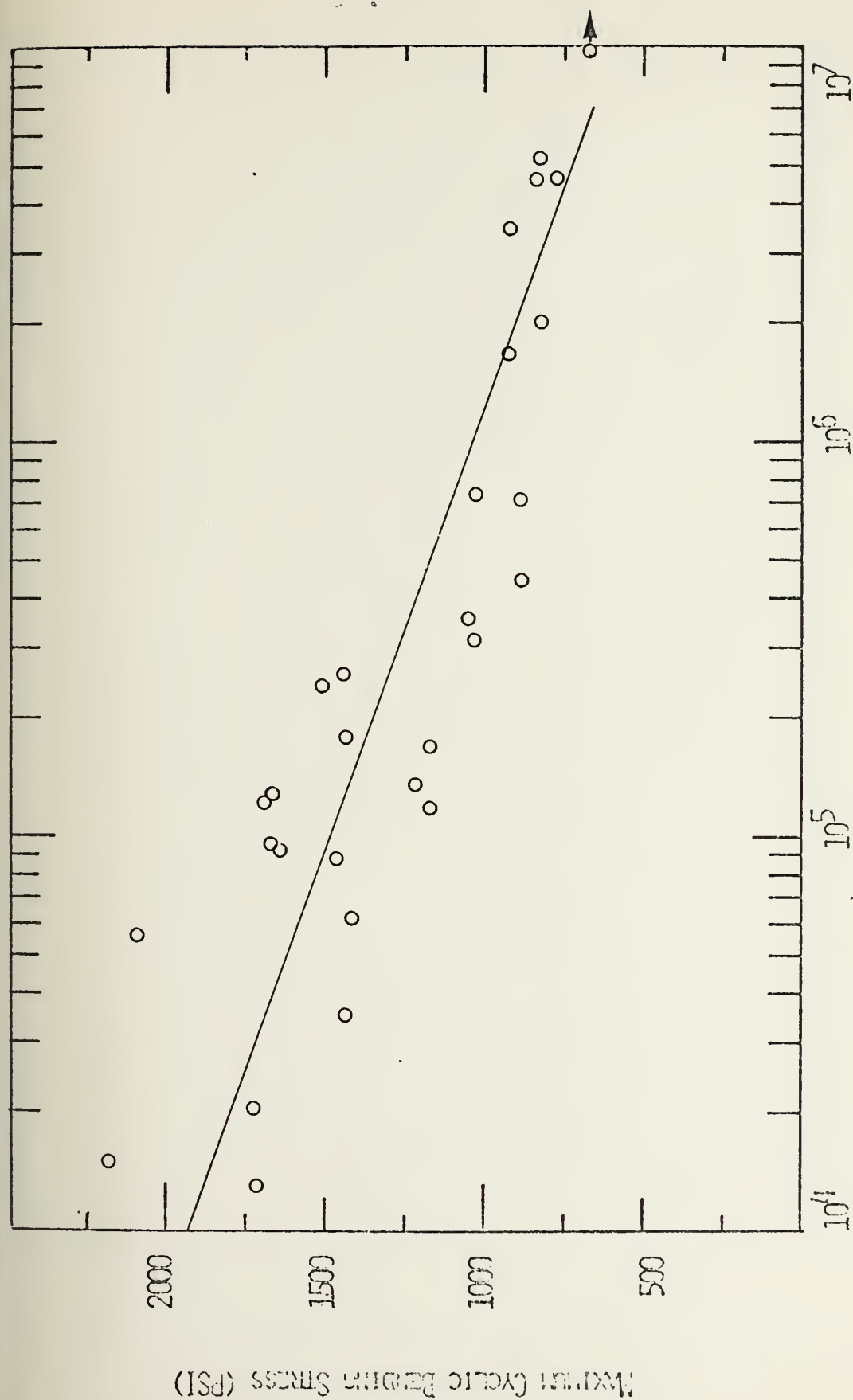


FIGURE 16. S-N PLOT FOR SERIES 1PSG





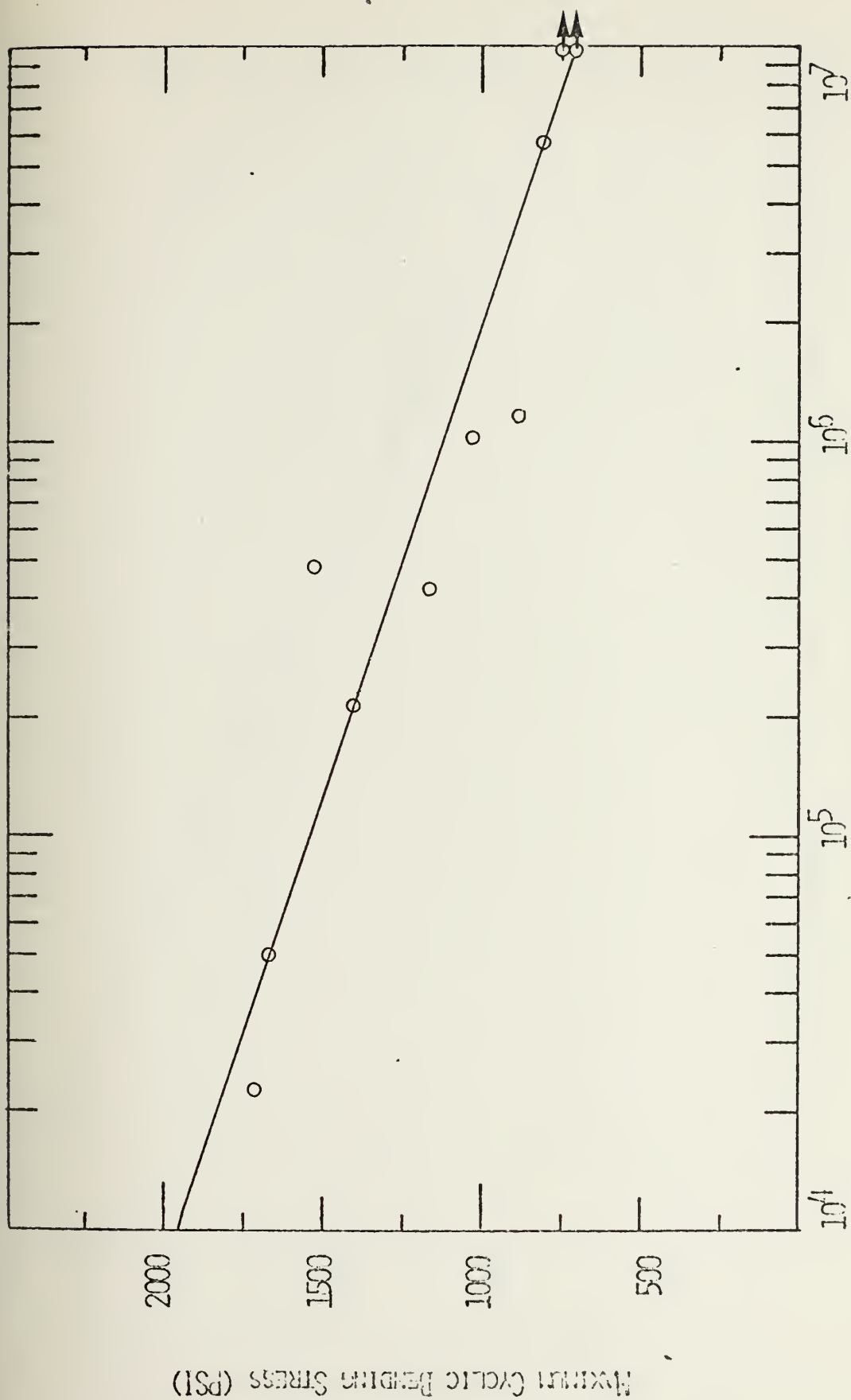


FIGURE 17. S-N PLOT FOR SERIES 4ESG



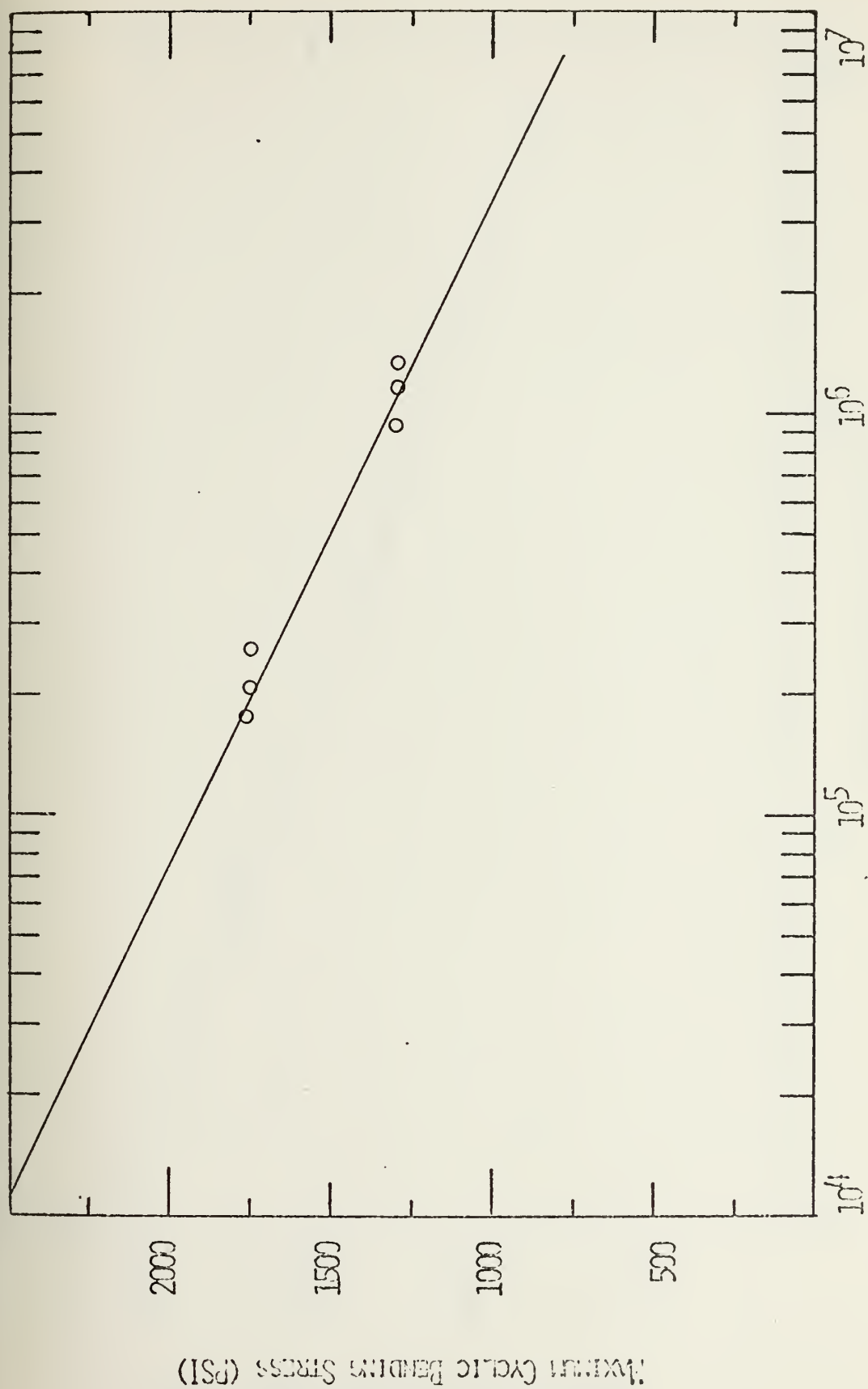


FIGURE 18. S-N PLOT FOR PANEL QUL7S3



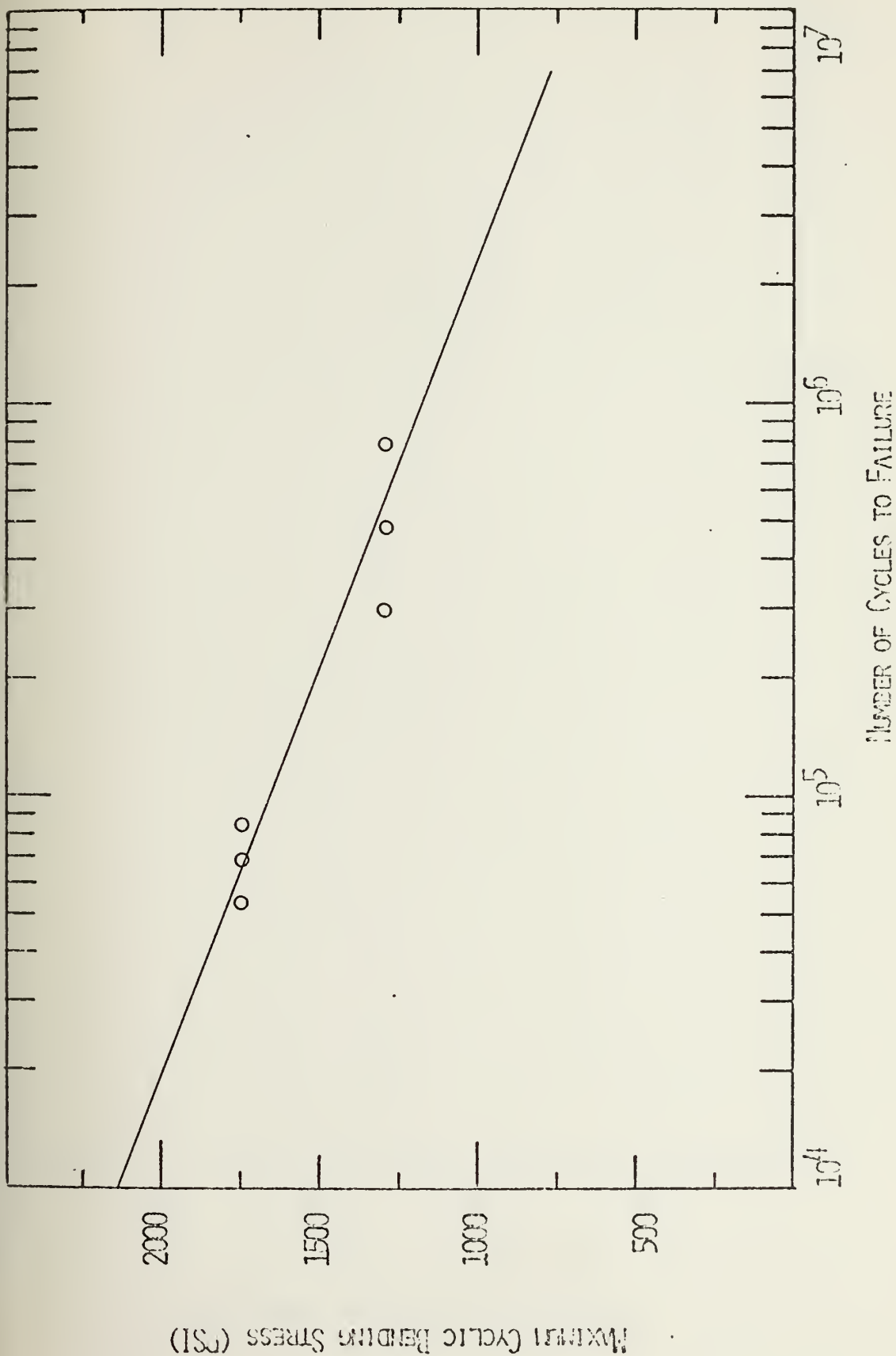


FIGURE 19. S-N PLOT FOR PANEL QUT7S2



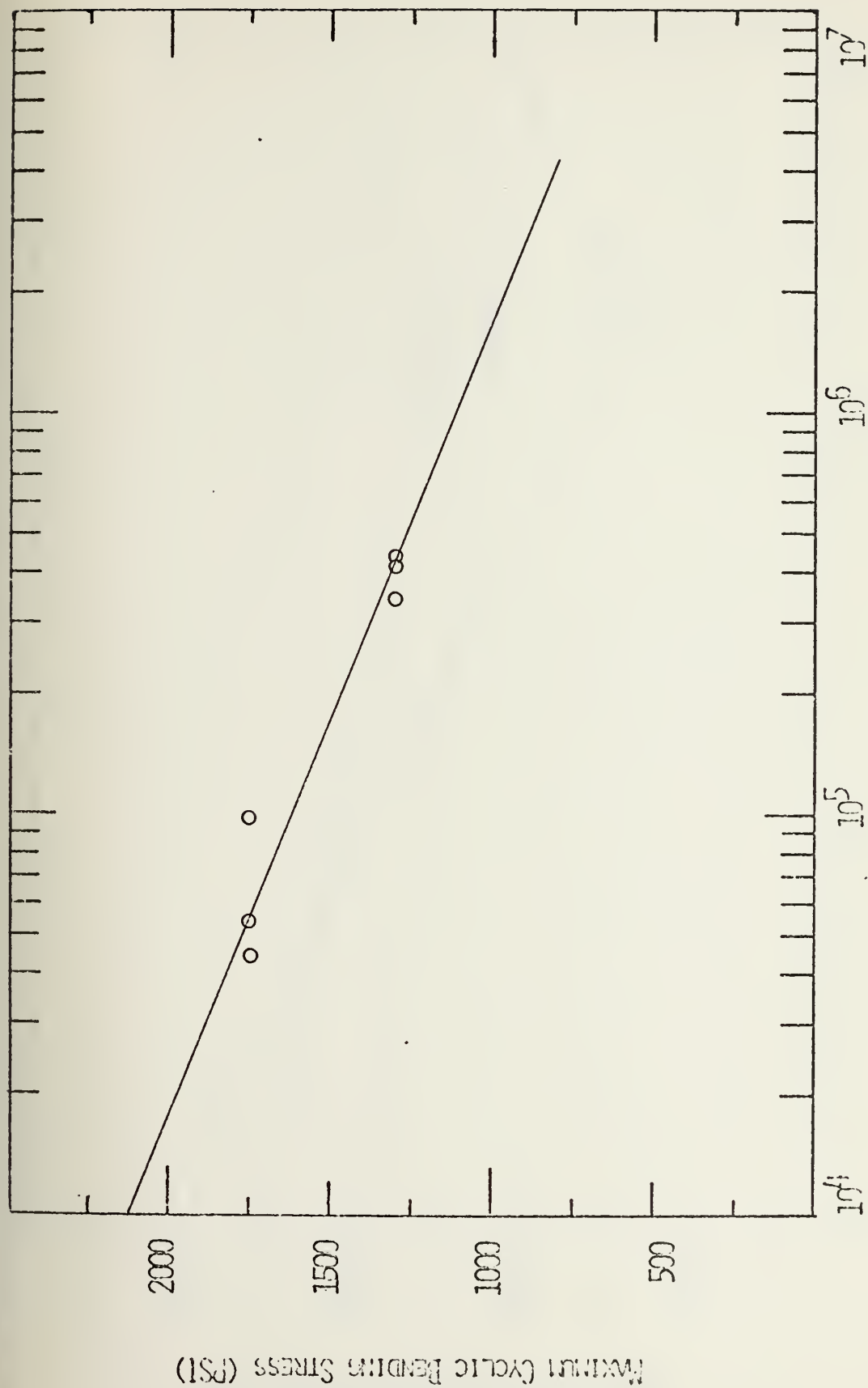


FIGURE 20. S-N PLOT FOR PANEL QUB7S1





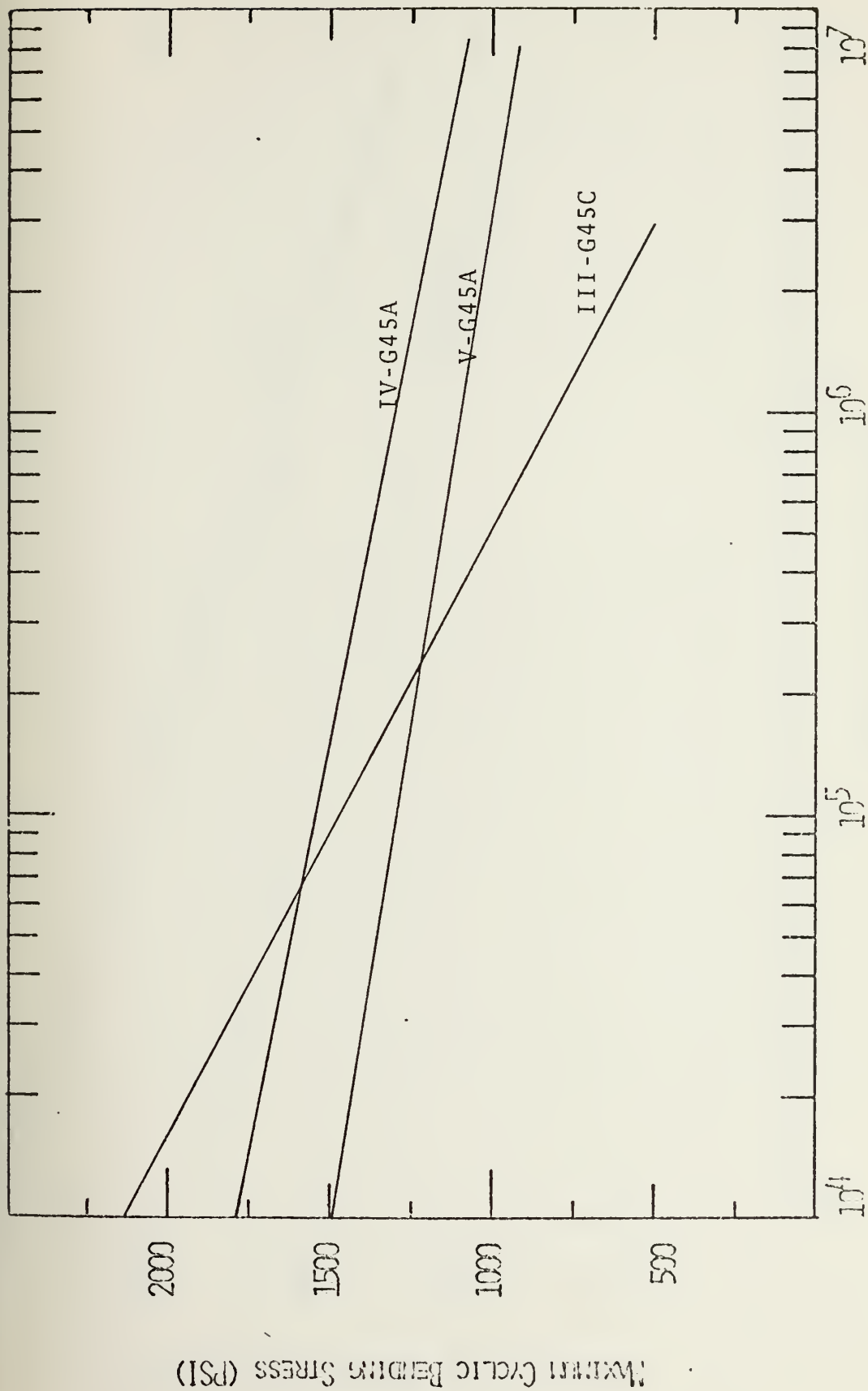
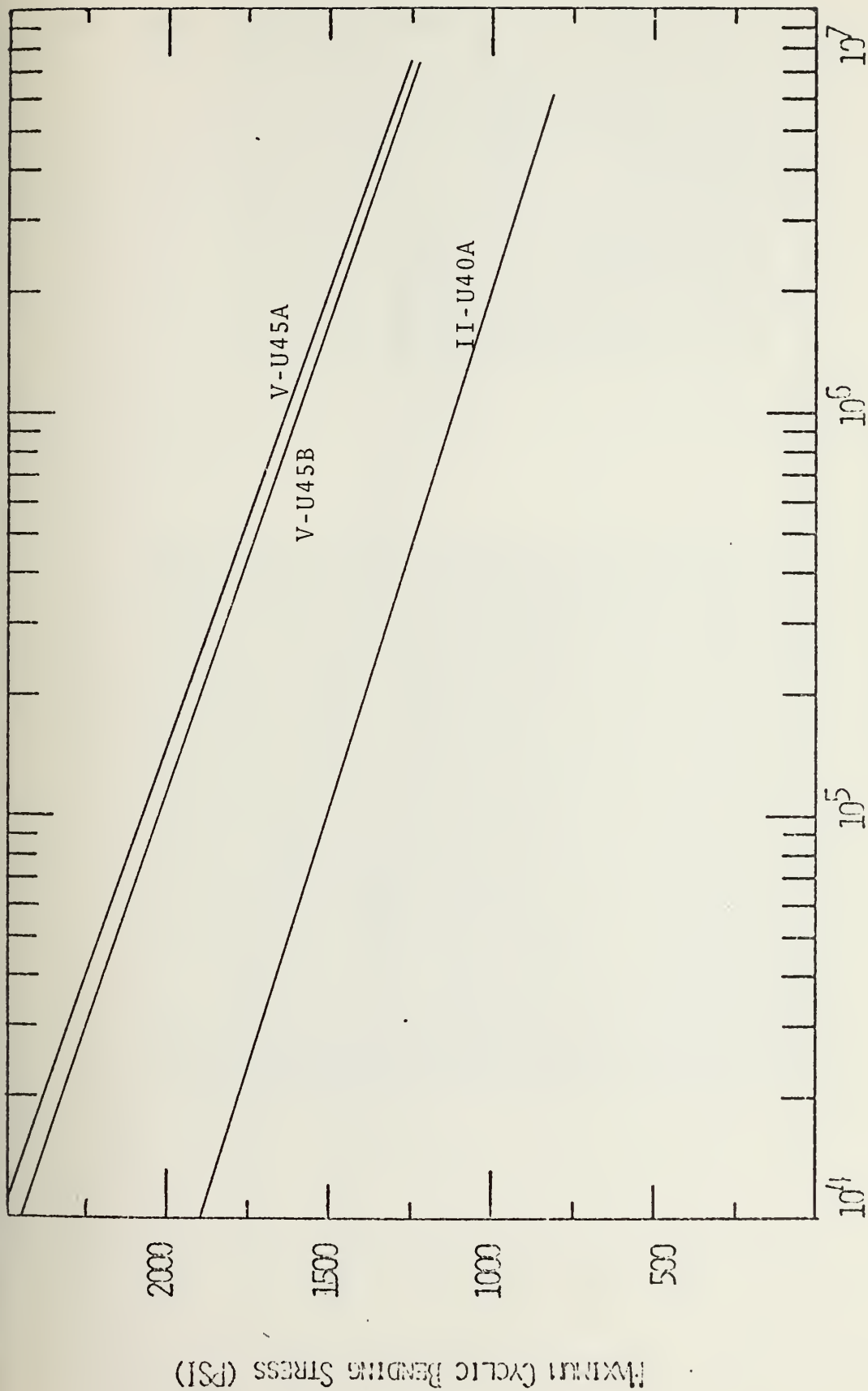


FIGURE 21. S-N PLOT COMPARING RESULTS OF PANELS IV-G45A, V-G45A, AND III-G45C

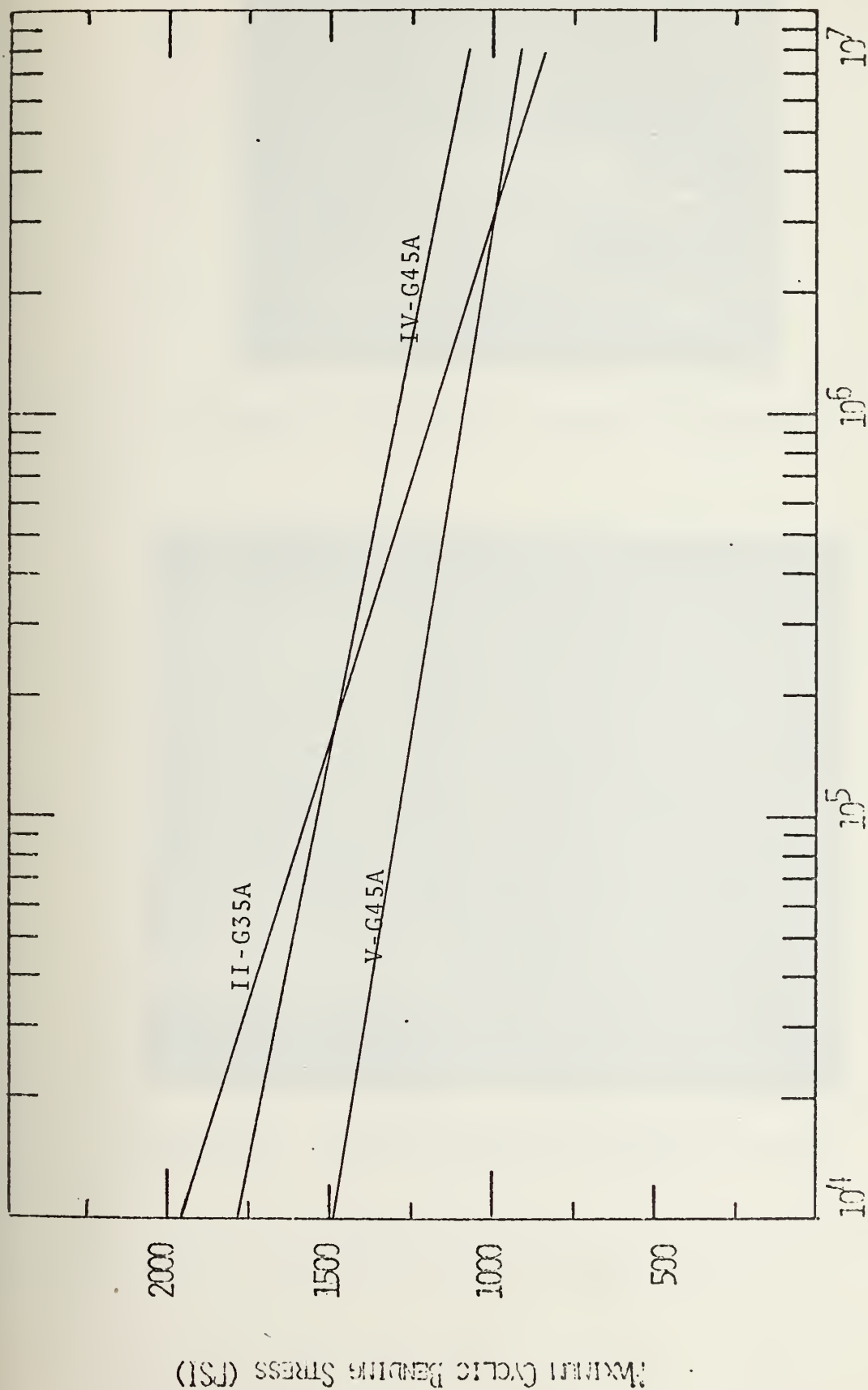




NUMBER OF CYCLES TO FAILURE

FIGURE 22. S-N PLOT COMPARING RESULTS OF PANELS V-U45A, V-U45B, AND II-U40A





NUMBER OF CYCLES TO FAILURE

FIGURE 23. S-N PLOT COMPARING RESULTS OF PANELS IV-G45A, V-G45A, AND II-G35A



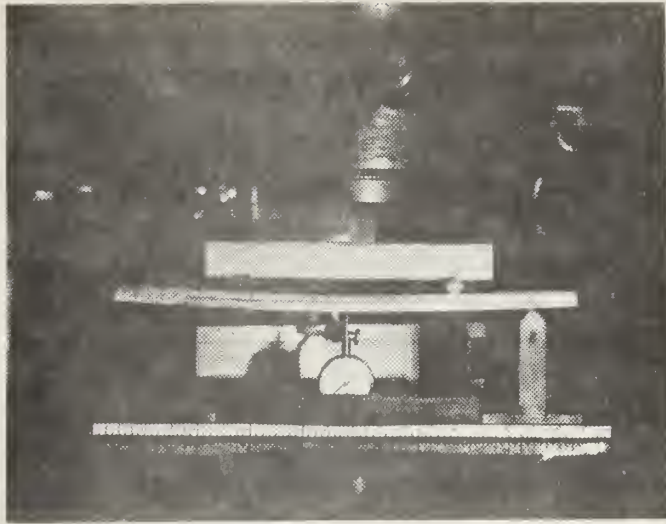


FIGURE 24. MONOTONIC BENDING APPARATUS

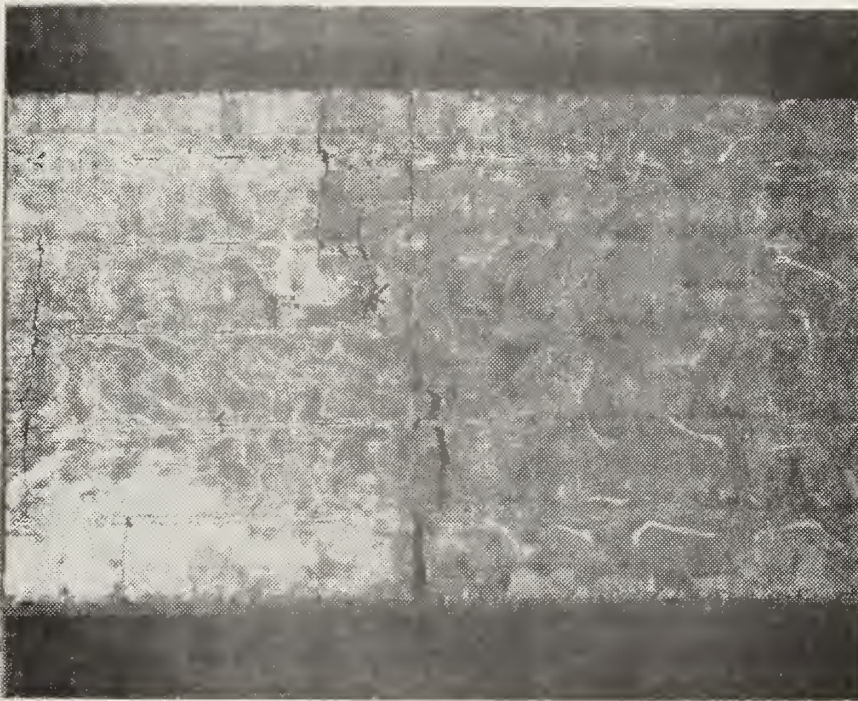


FIGURE 25. TYPICAL MONOTONIC BENDING FAILURE





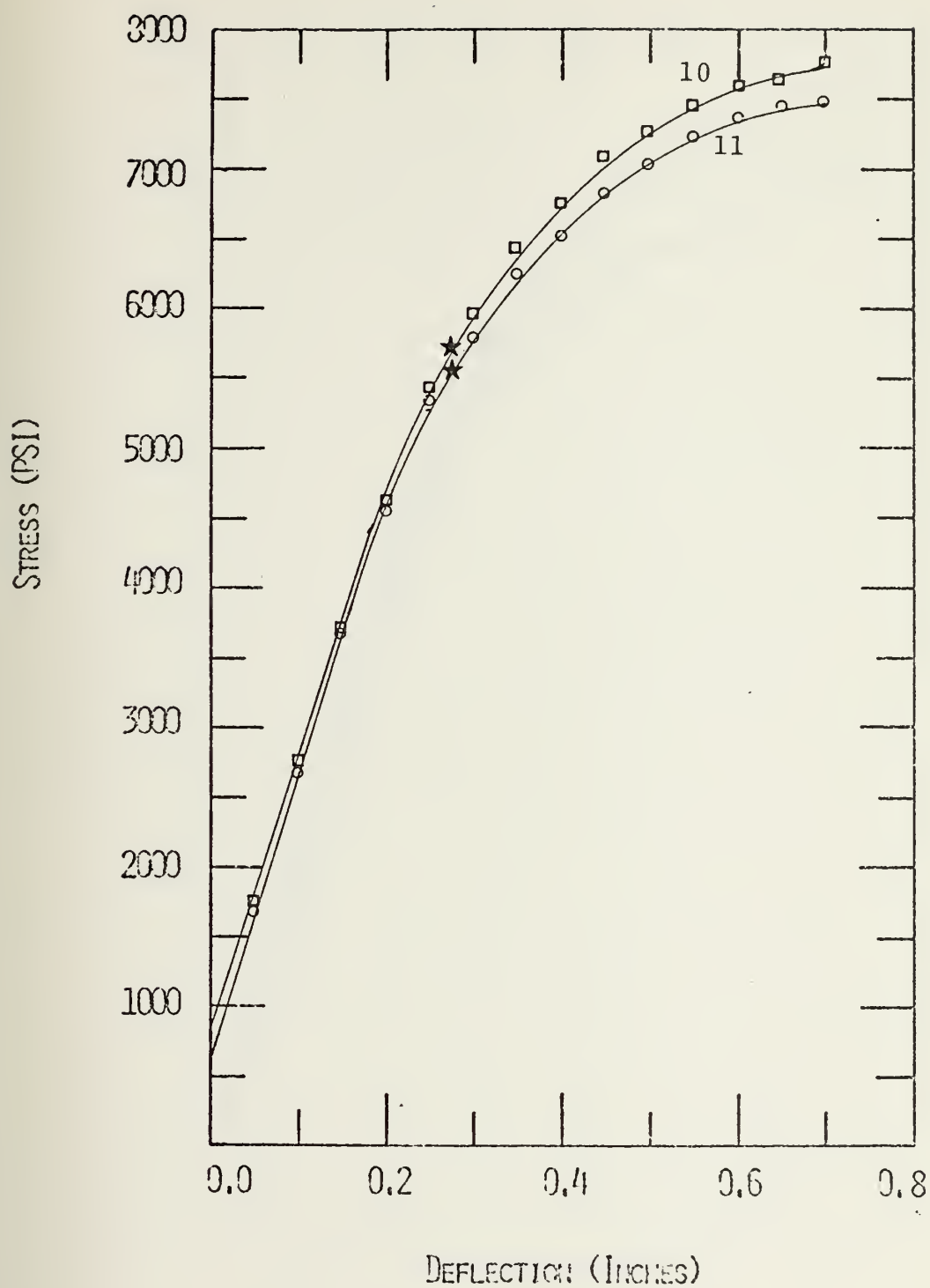


FIGURE 26. STRESS-DEFLECTION CURVES FOR SPECIMENS V-U45B-10 AND V-U45B-11 (NO PRECYCLING)



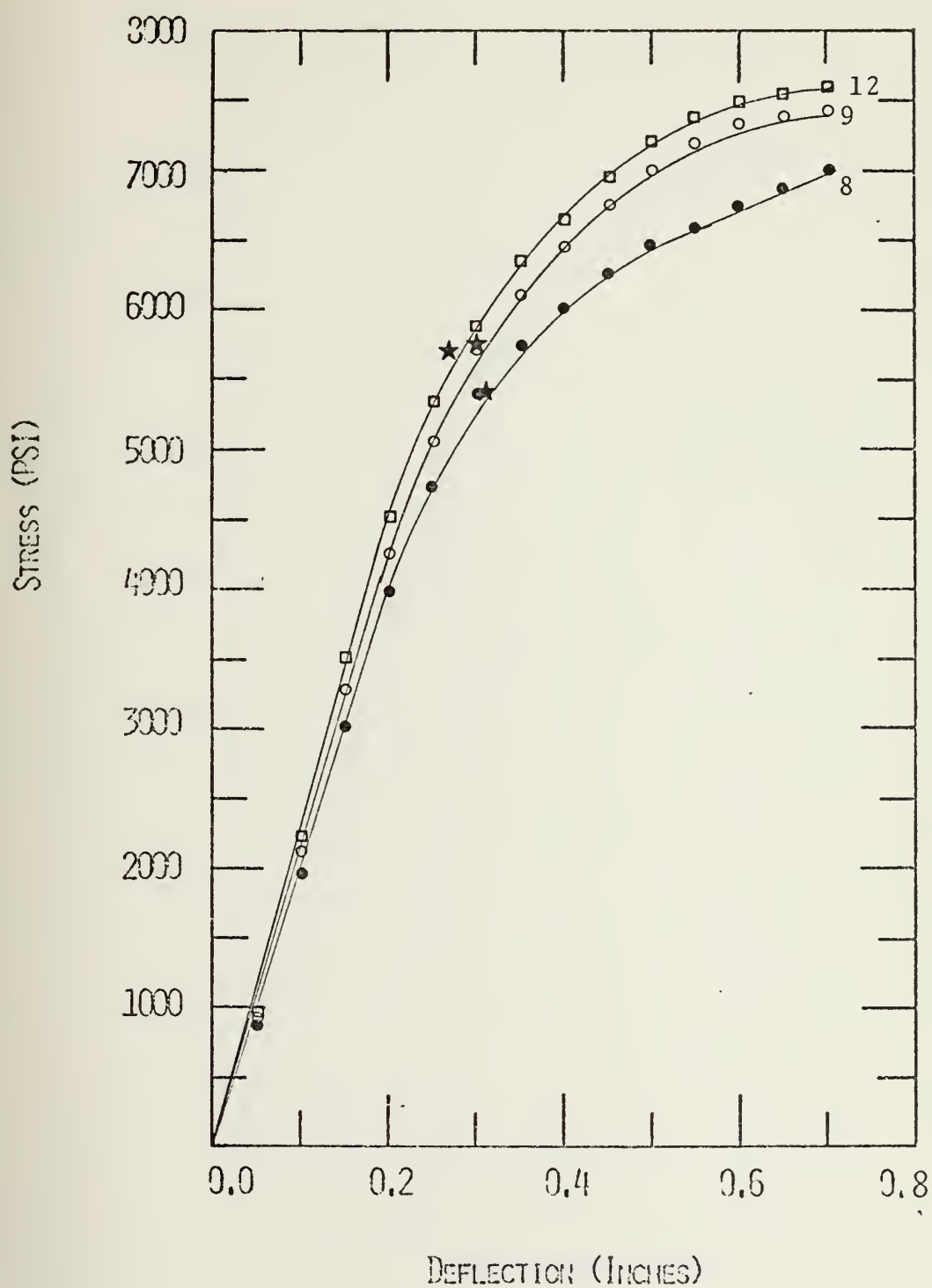


FIGURE 27. STRESS-DEFLECTION CURVES FOR SPECIMENS V-U45B-8, V-U45B-9, AND V-U45B-12 (33% PRECYCLING)



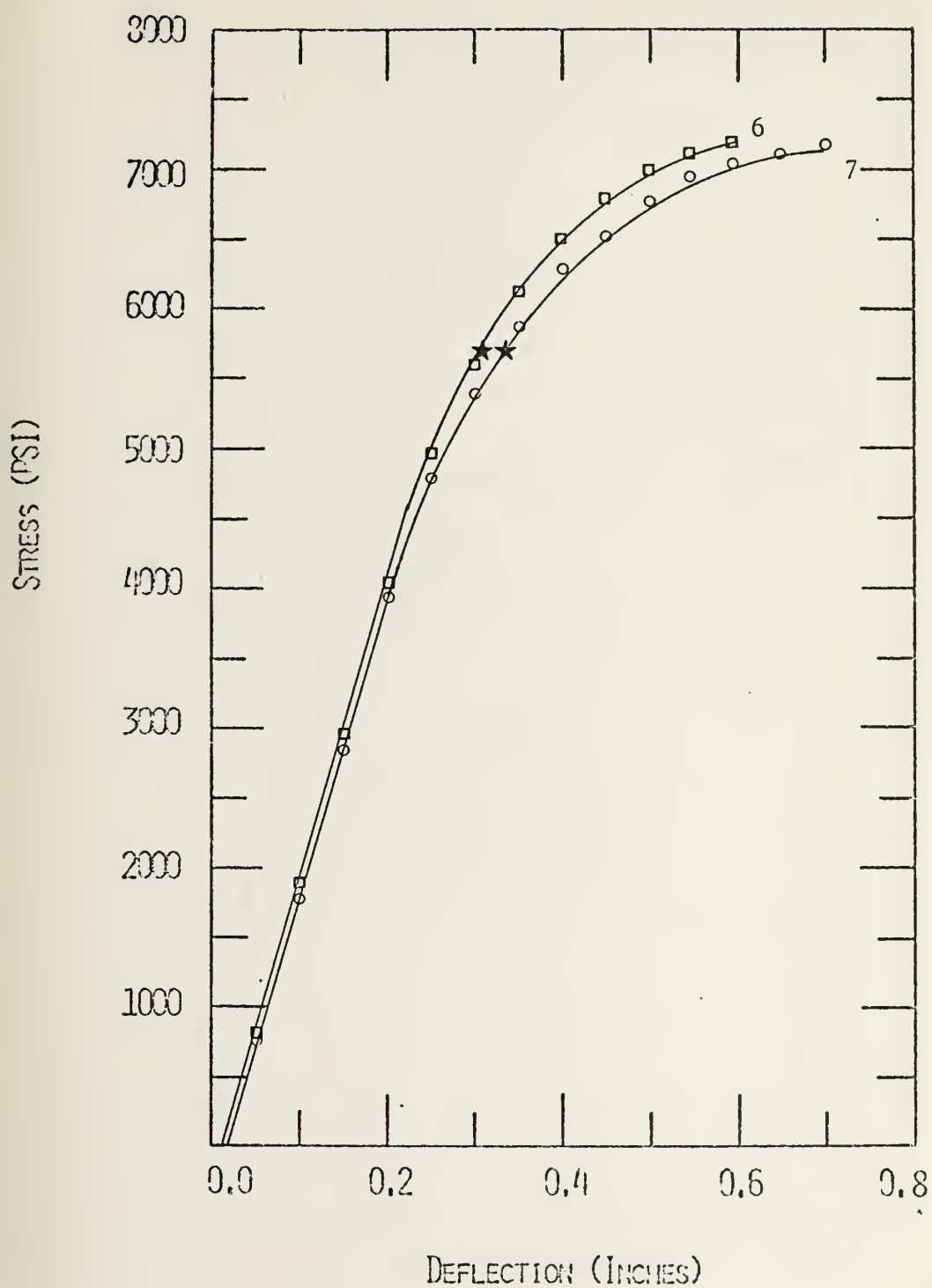


FIGURE 28. STRESS-DEFLECTION CURVES FOR SPECIMENS V-U45B-6 AND V-U45B-7 (66% PRECYCLING)



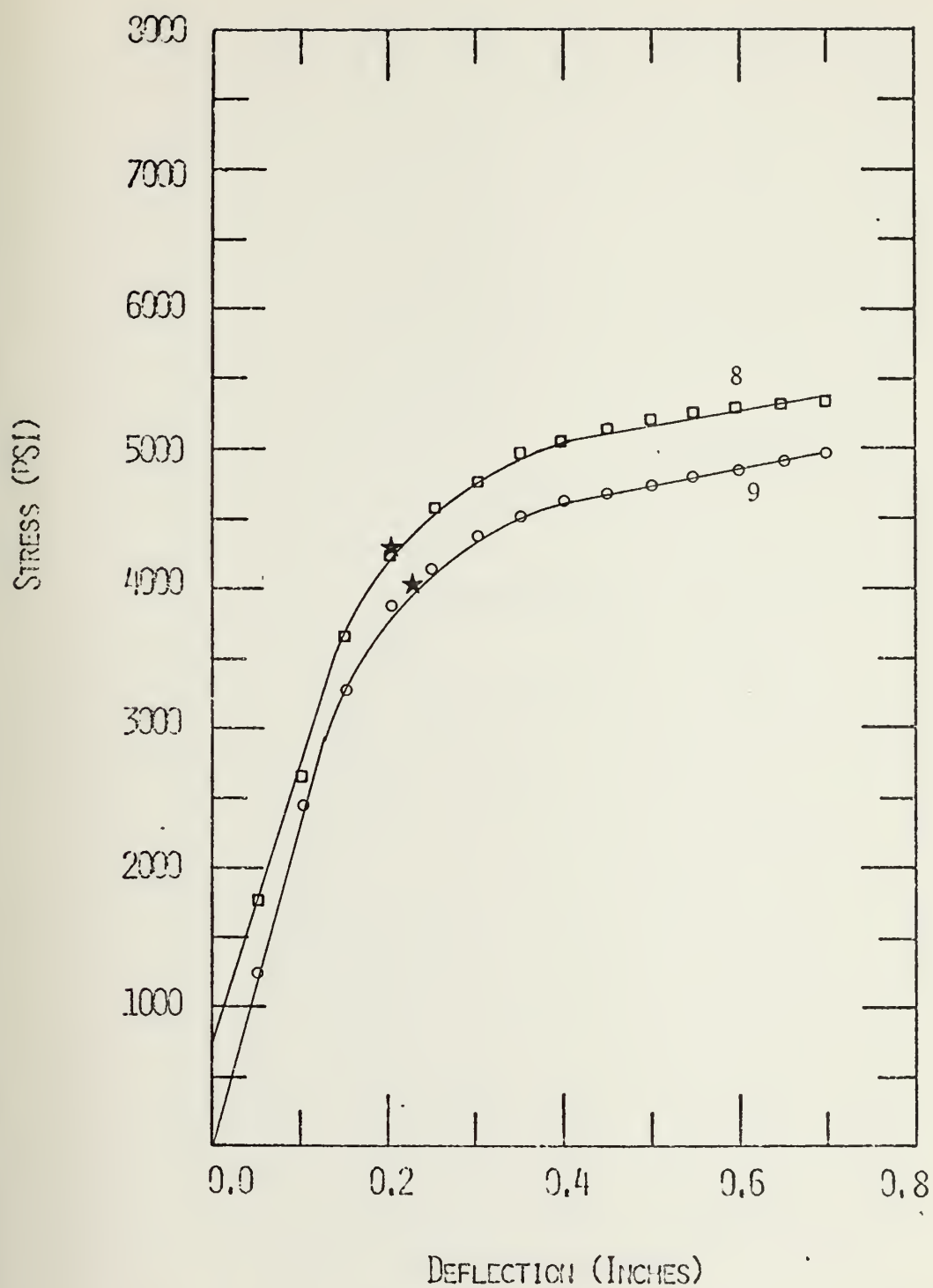


FIGURE 29. STRESS-DEFLECTION CURVES FOR SPECIMENS V-G45A-8 AND V-G45A-9 (NO PRECYCLING)





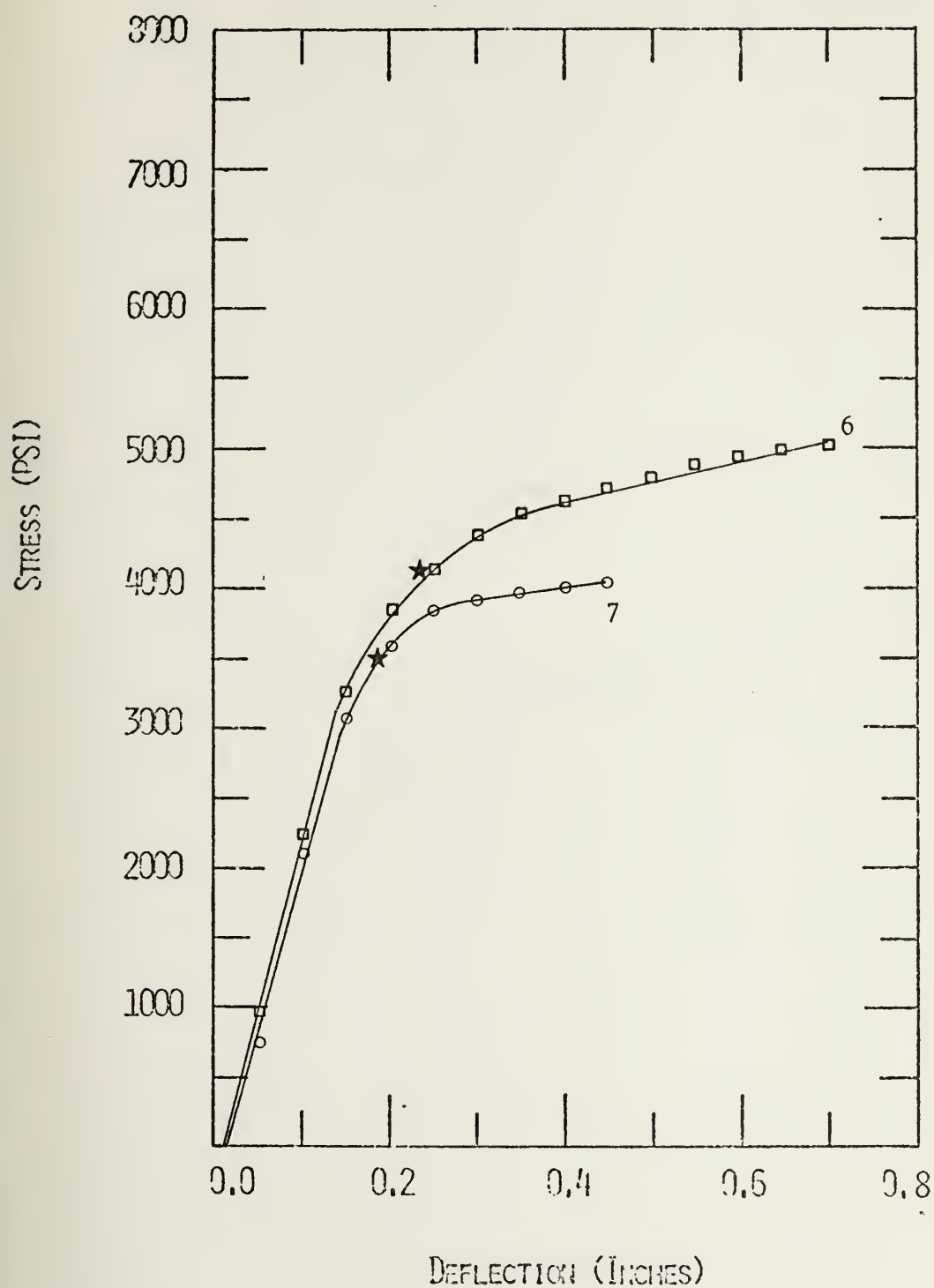


FIGURE 30. STRESS-DEFLECTION CURVES FOR SPECIMENS V-G45A-6 AND V-G45A-7 (33% PRECYCLING)



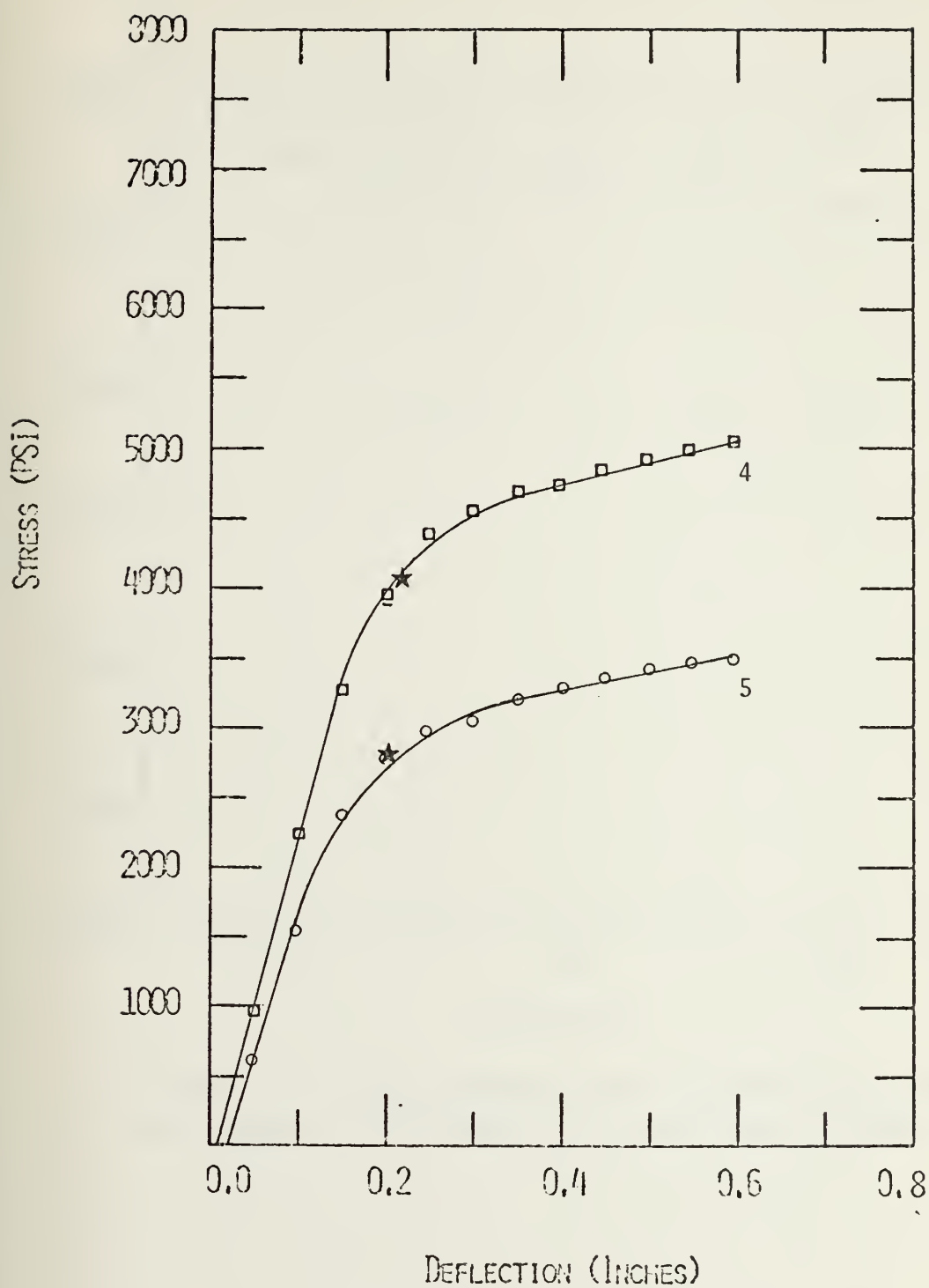


FIGURE 31. STRESS-DEFLECTION CURVES FOR SPECIMENS V-G45A-4 AND V-G45A-5 (66% PRECYCLING)



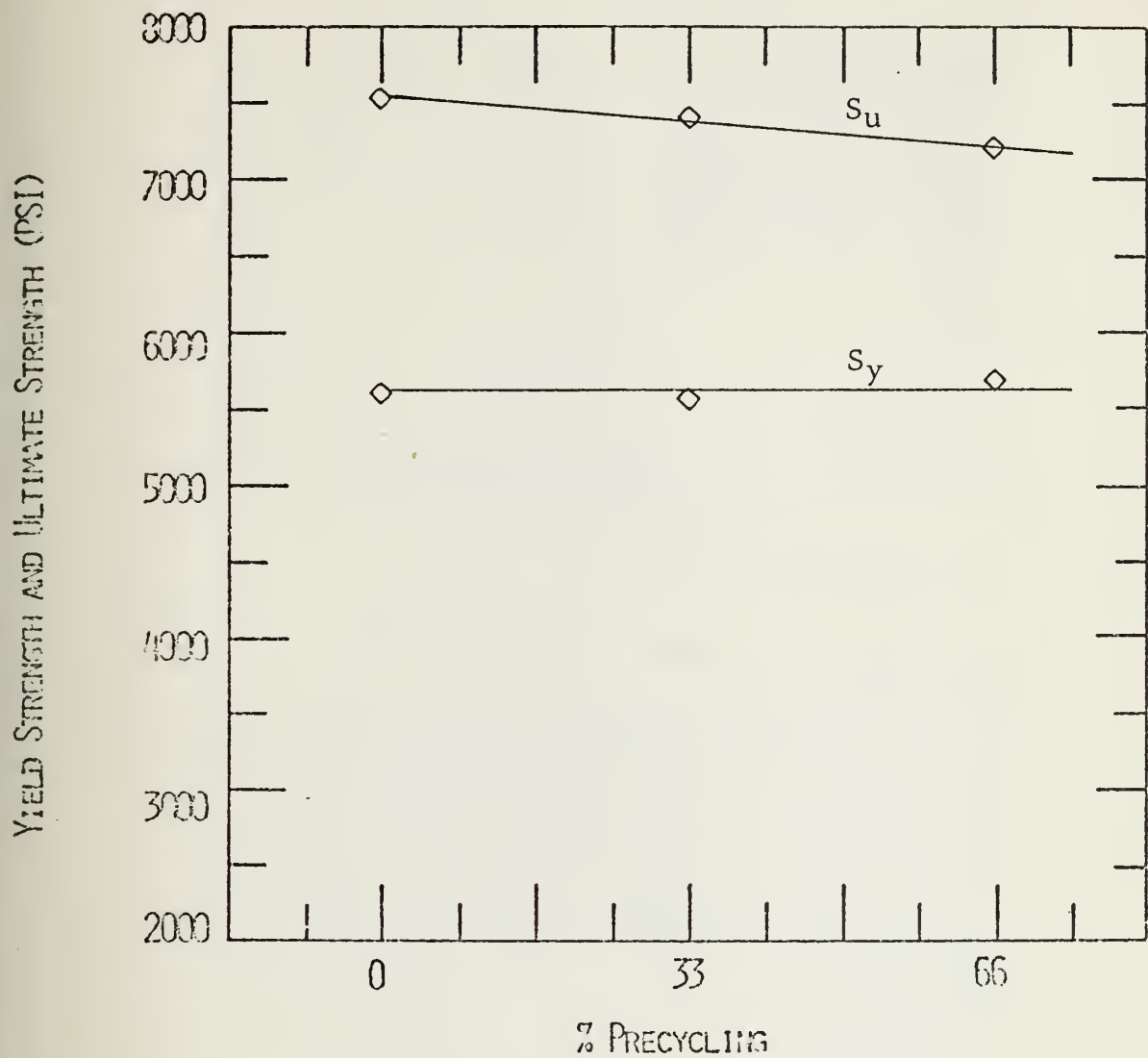


FIGURE 32. YIELD STRENGTH AND ULTIMATE STRENGTH VS. PERCENTAGE OF PRECYCLING FOR PANEL V-U45B



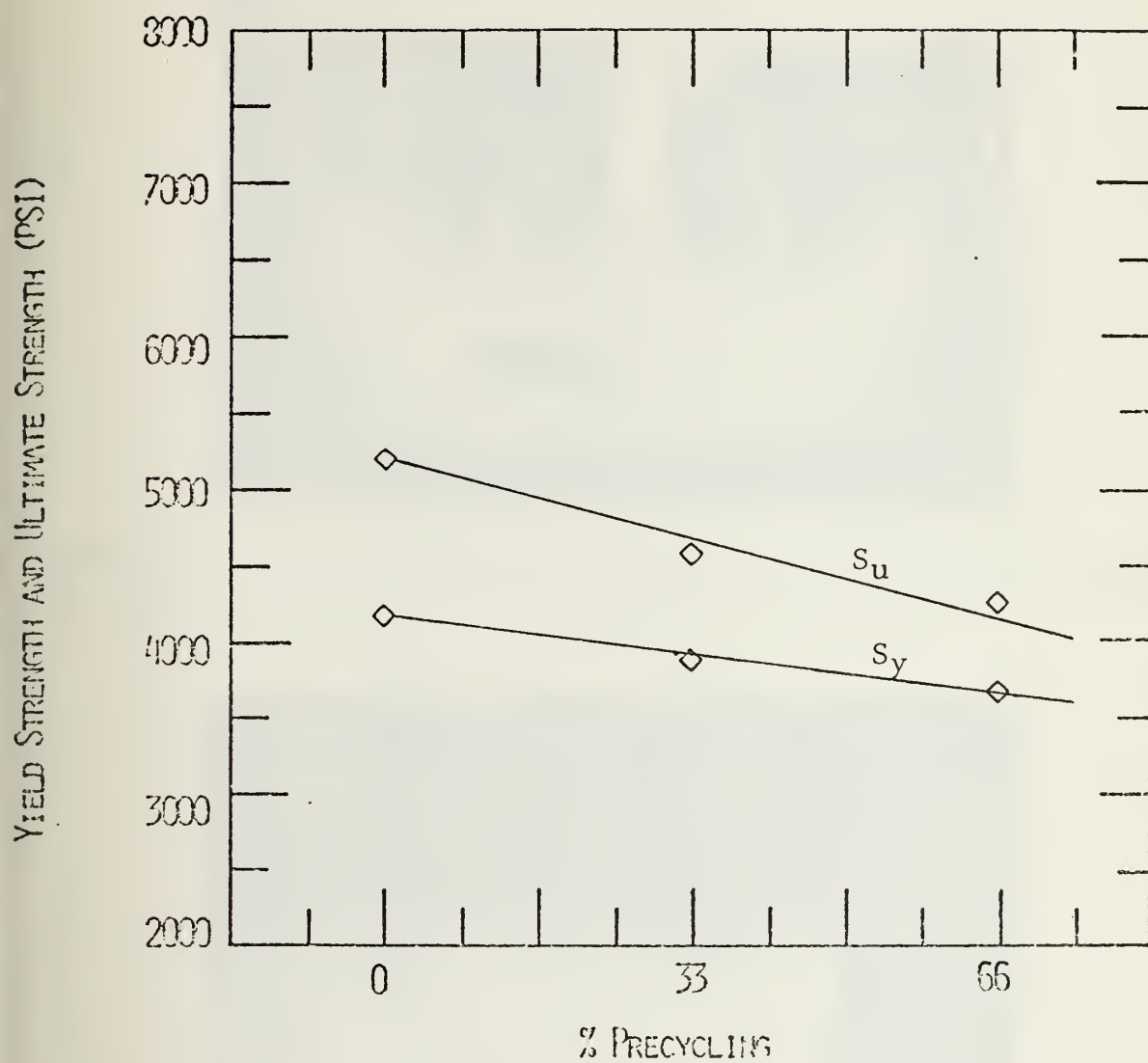


FIGURE 33. YIELD STRENGTH AND ULTIMATE STRENGTH VS. PERCENTAGE OF PRECYCLING FOR PANEL V-G45A





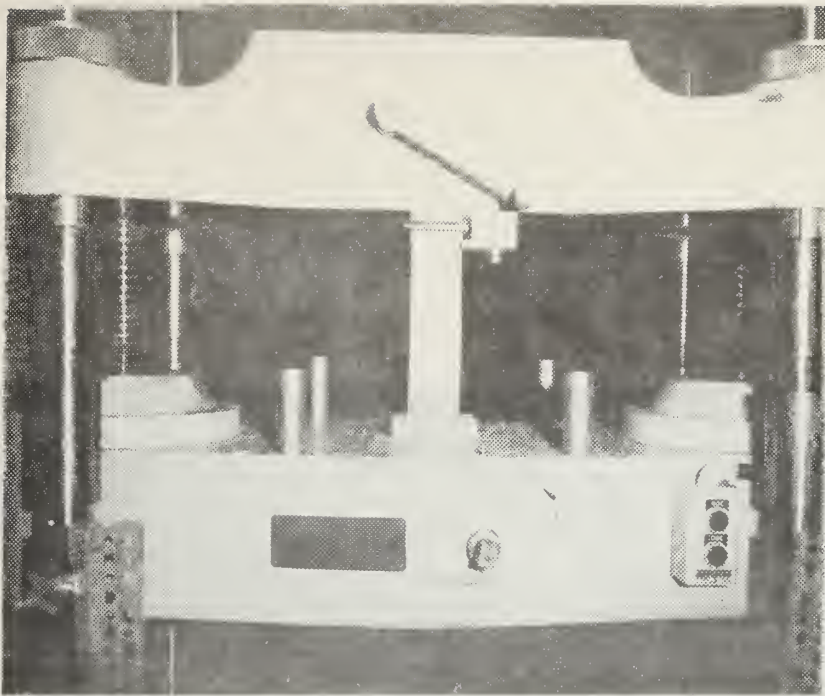


FIGURE 34. TINIUS-OLSEN TESTING MACHINE WITH TENSILE SPECIMEN IN PLACE

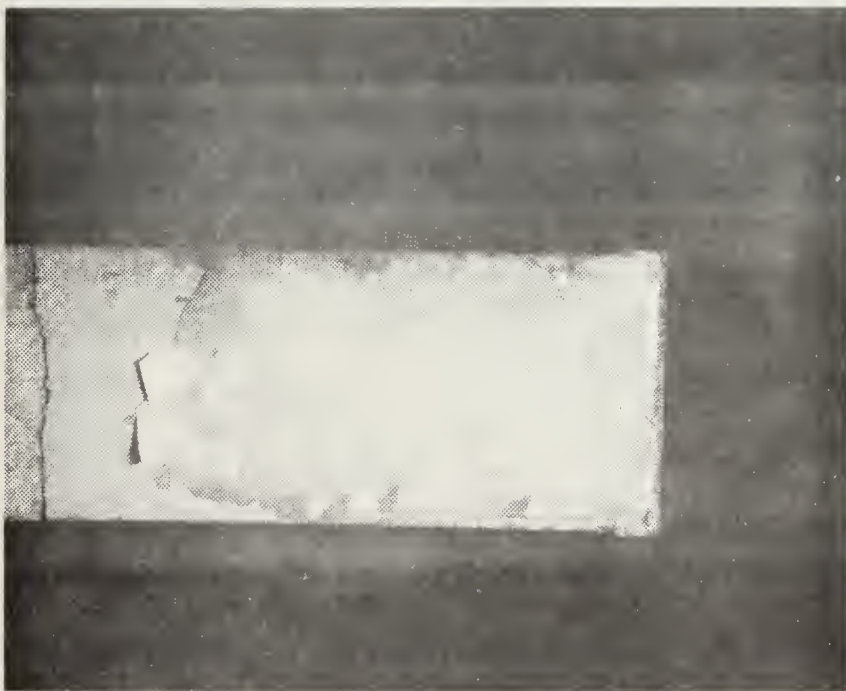


FIGURE 35. TENSILE SPECIMEN SHOWING EPOXY/PAPER COATING AND TENSILE FAILURE CRACK





FIGURE 36. UNUSUAL 3-PLANE TENSILE FAILURE



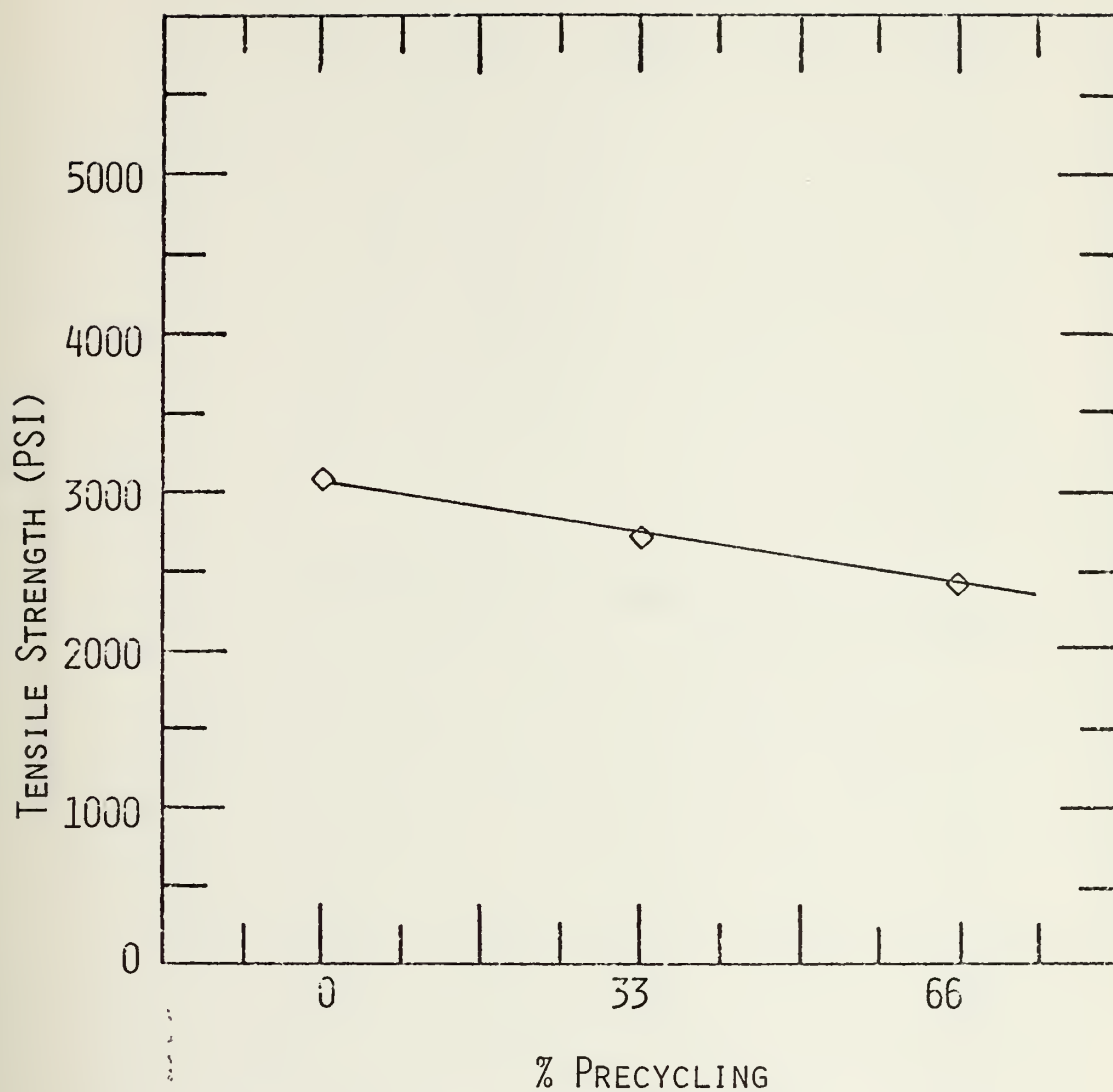


FIGURE 37. TENSILE STRENGTH VS. PERCENTAGE OF PRECYCLING FOR PANEL V-U45A



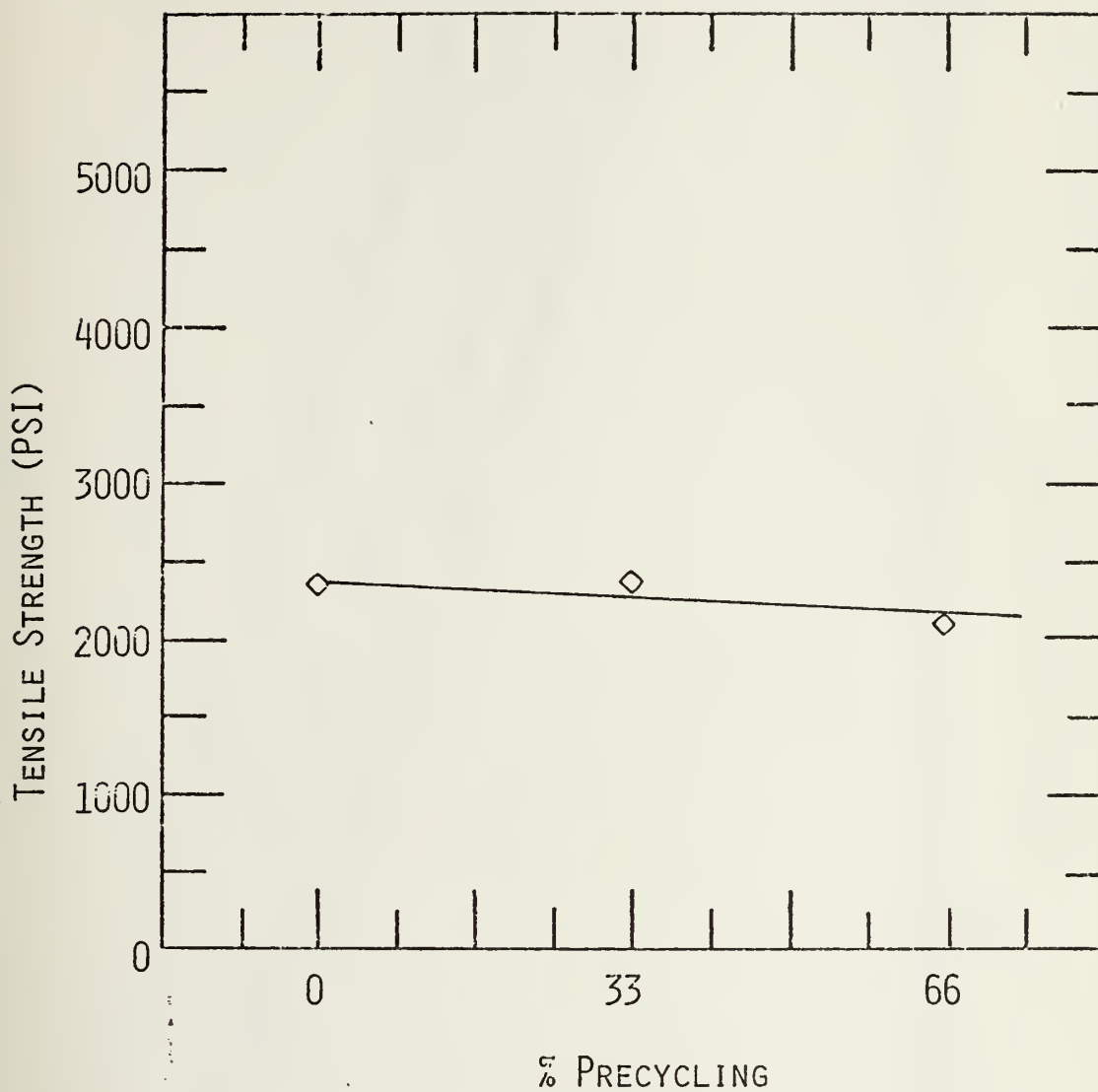
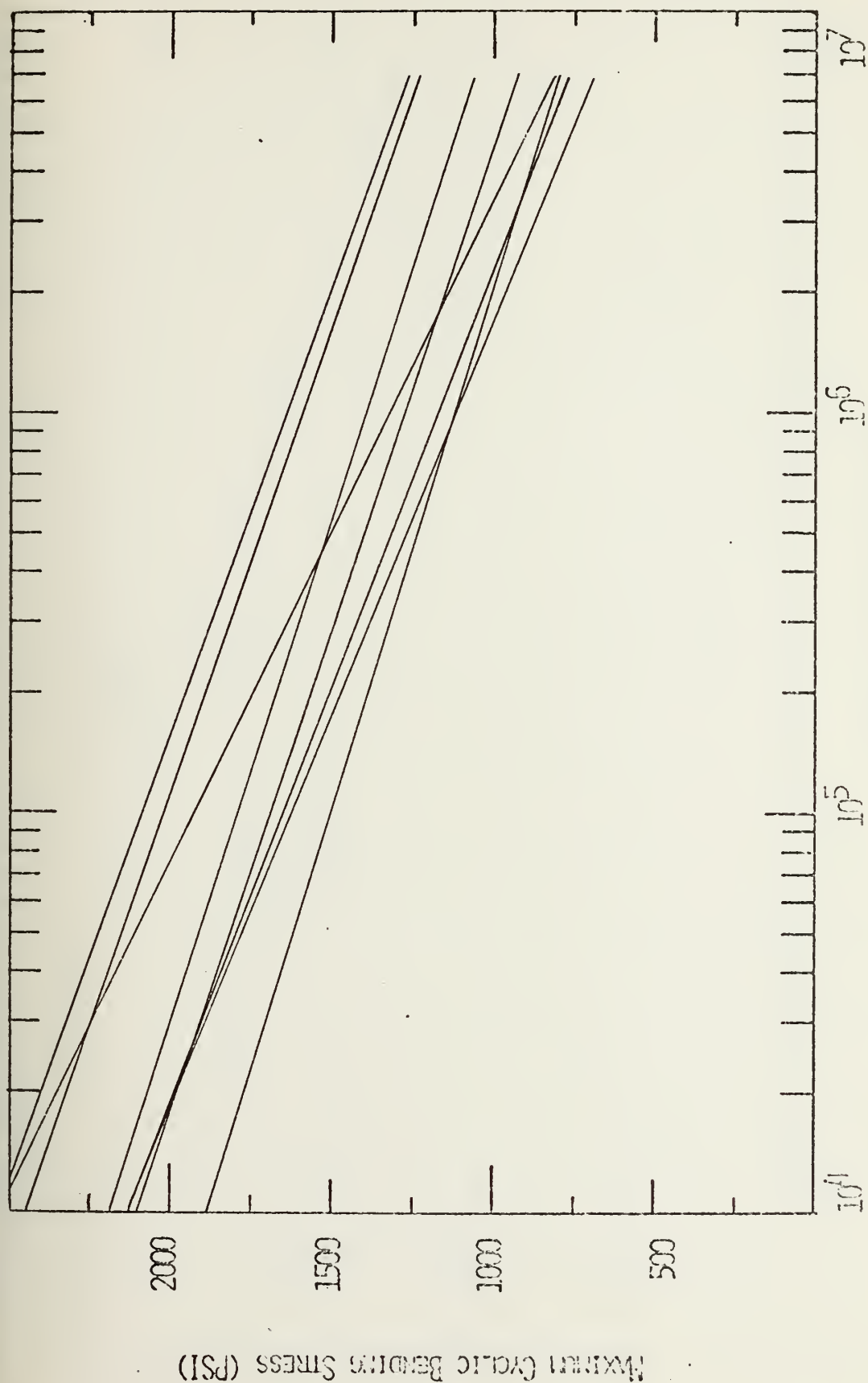


FIGURE 38. TENSILE STRENGTH VS. PERCENTAGE OF PRECYCLING FOR PANEL IV-G45A







NUMBER OF CYCLES TO FAILURE

FIGURE 39. S-N PLOT COMPARING RESULTS OF ALL PANELS WITH UNGALVANIZED WIRE REINFORCEMENT



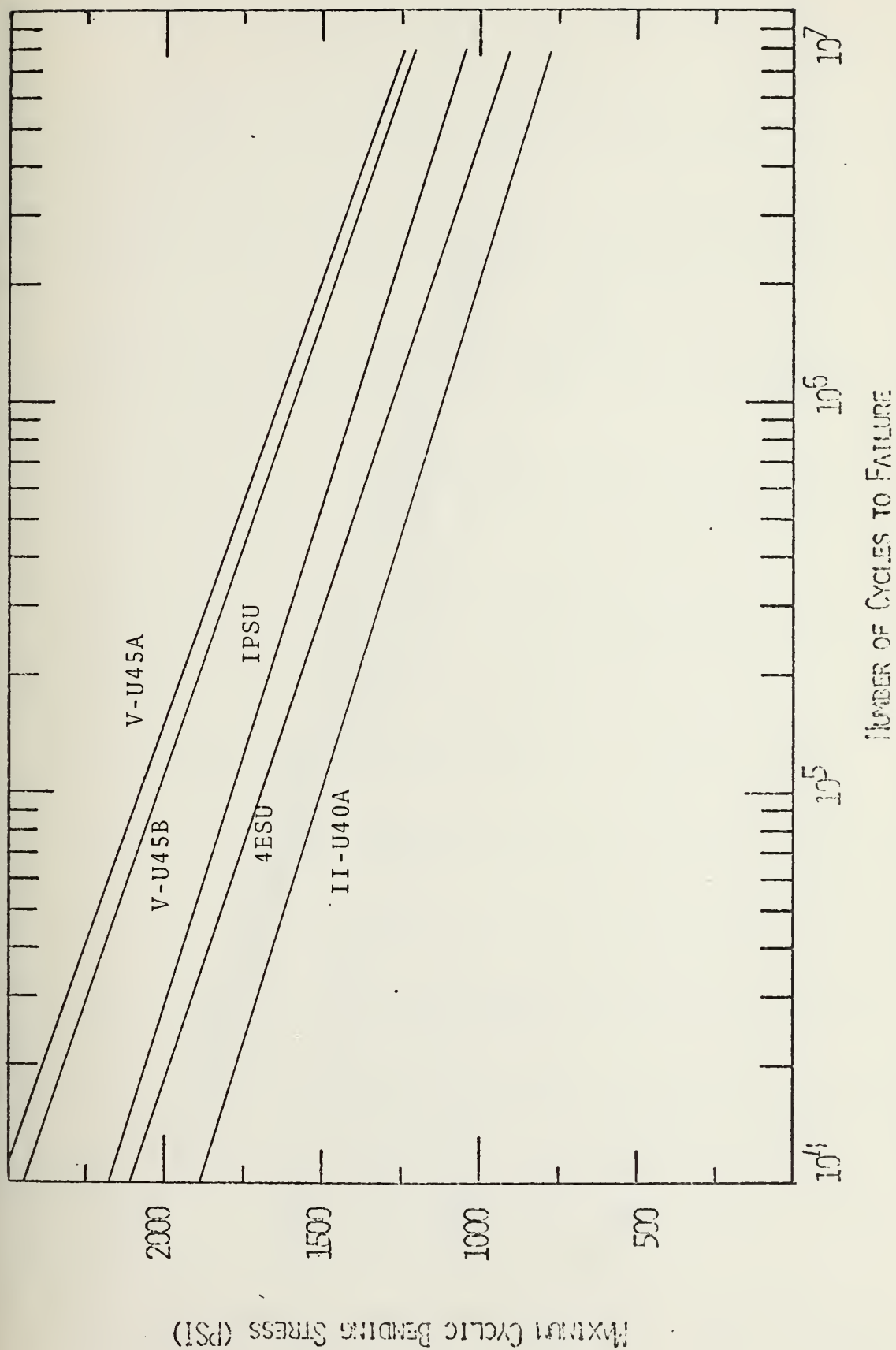


FIGURE 40. S-N PLOT COMPARING RESULTS OF PANELS V-U45A, V-U45B, II-U40A, IPSU, AND 4ESU.



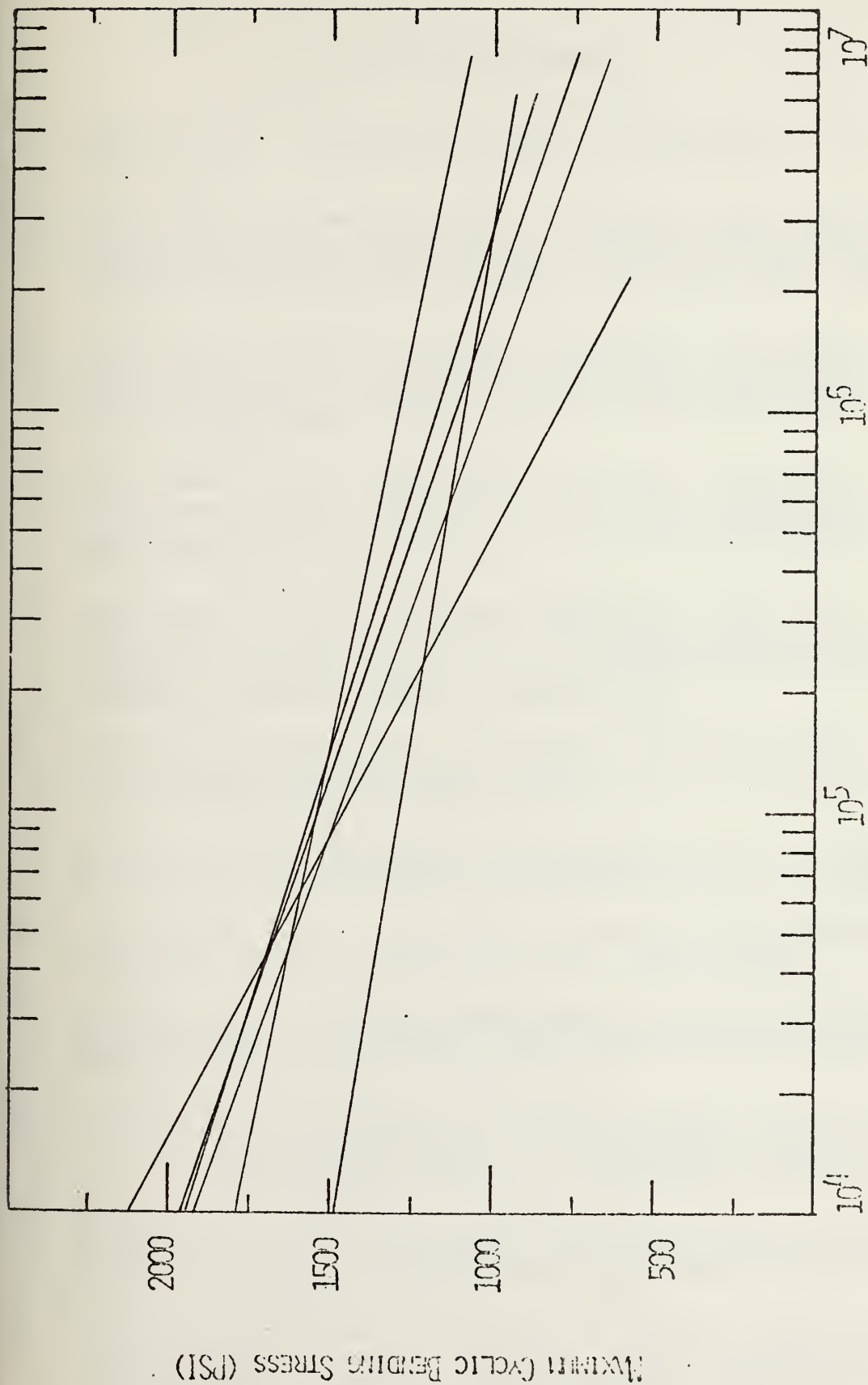


FIGURE 41. S-N PLOT COMPARING RESULTS FOR ALL PANELS WITH GALVANIZED WIRE REINFORCEMENT



## LIST OF REFERENCES

1. Hurd, M. K., "Ferrocement Boats," ACI Journal, p. 202-204, March 1969.
2. Department of the Environment (Canada), Industrial Development Branch Report No. 52, An Introduction to Design for Ferro-Cement Vessels, by G. W. Bigg, January 1972.
3. Department of the Environment (Canada), Industrial Development Branch Report No. 42, Ferro-Cement for Canadian Fishing Vessels, compiled and edited by W. G. Scott, August 1971.
4. Department of the Environment (Canada), Industrial Development Branch Report No. 48, Ferro-Cement for Canadian Fishing Vessels, V. 2, by A. W. Greenius and John D. Smith, August 1972.
5. Department of the Environment (Canada), Industrial Development Branch Report No. 55, Ferro-Cement for Canadian Fishing Vessels, V. 3, prepared by the British Columbia Research Council, August 1972.
6. Naval Civil Engineering Laboratory Technical Note N-1341, Ferro-Cement Construction Panels, by H. H. Haynes and G. S. Guthrie, April 1974.
7. Simpson, M. G., Fatigue of Ferro-Cement, M.S. & Engr. Thesis, Naval Postgraduate School, Monterey, California, June 1974.
8. B zukladov, V. F., and others, Ship Hulls Made of Reinforced Concrete, Navships Translation No. 1148, 1968.
9. Sargent, D. P., Factors Effecting the Fatigue Strength of Ferro-Cement, M.S. Thesis, Naval Postgraduate School, Monterey, California, December 1974.
10. University of California (Berkeley) Report No. UC SESM 71-14, Solving the Galvanic Cell Problem in Ferro-Cement, by K. A. Christiansen and R. B. Williamson, July 1971.
11. Annual Book of American Society for Testing and Materials Standards, Part 14, Concrete and Mineral Aggregates; Manual of Concrete Testing, November 1974.
12. The Society of Naval Architects and Marine Engineers Technical and Research Report No. R-14, References on Ferro-Cement in the Marine Environment, prepared by Task Group HS-6-4, October 1972.





13. Dorn, W. S. and McCracken, D. D., Numerical Methods with Fortran IV Case Studies, p. 310-317, Wiley, 1972.
14. Kline, S. J. and McClintock, F. A., "Describing Uncertainties in Single Sample Experiments," Mechanical Engineering, p. 3-8, January 1953.



# INITIAL DISTRIBUTION LIST

	No. Copies
1. Defense Documentation Center Cameron Station Alexandria, Virginia 22314	2
2. Library, Code 0212 Naval Postgraduate School Monterey, California 93940	2
3. Asst. Professor E. A. McKinnon, Code 59Mz Department of Mechanical Engineering Naval Postgraduate School Monterey, California 93940	10
4. ENS Earle S. Babcock, USN 7634 Prairie Mound Way San Diego, California 92139	1
5. Harvey Haynes Ocean Structures Division Naval Civil Engineering Laboratory Port Hueneme, California 93041	1
6. Frank E. Brauer Laboratory for Advanced Composites Naval Ship Research and Development Center Annapolis, Maryland 21402	1
7. Dr. Kenneth Saczalski, Code 439 Office of Naval Research 800 North Quincy Arlington, Virginia 22217	1
8. Professor Tom Butler Mechanical Engineering Department U.S. Naval Academy Annapolis, Maryland 21402	1
9. LCDR Michael G. Simpson, USN Navy Section, MAAG, Republic of China Box 12 APO San Francisco, California 96263	1
10. LT David P. Sargent, USN USS SHAKORI (ATF-162) FPO New York, New York 09501	1



11. Mechanical Engineering Dept. Library, Code 59 1  
Naval Postgraduate School  
Monterey, California 93940









Thesis  
B1051  
c.1

Babcock

The effects of  
precycling on the  
strength of ferrocement.

160999

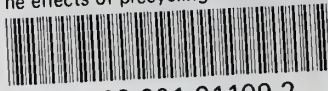
Thesis

B1051 Babcock  
c.1

The effects of  
precycling on the  
strength of ferrocement.

160999

thesB1051  
The effects of precycling on the strengt



3 2768 001 91109 2  
DUDLEY KNOX LIBRARY